

## Modeling Biologically Important NH...# Interactions Using peri-Disubstituted Naphthalenes

Alexander F. Pozharskii, Olga V. Dyablo, Olga G. Pogosova, Valery A. Ozeryanskii,  
Aleksander Filarowski, Kseniya M. Vasilikhina, and Narek A. Dzhangiryan

*J. Org. Chem.*, **Just Accepted Manuscript** • DOI: 10.1021/acs.joc.0c01697 • Publication Date (Web): 10 Sep 2020

Downloaded from pubs.acs.org on September 12, 2020

### Just Accepted

“Just Accepted” manuscripts have been peer-reviewed and accepted for publication. They are posted online prior to technical editing, formatting for publication and author proofing. The American Chemical Society provides “Just Accepted” as a service to the research community to expedite the dissemination of scientific material as soon as possible after acceptance. “Just Accepted” manuscripts appear in full in PDF format accompanied by an HTML abstract. “Just Accepted” manuscripts have been fully peer reviewed, but should not be considered the official version of record. They are citable by the Digital Object Identifier (DOI®). “Just Accepted” is an optional service offered to authors. Therefore, the “Just Accepted” Web site may not include all articles that will be published in the journal. After a manuscript is technically edited and formatted, it will be removed from the “Just Accepted” Web site and published as an ASAP article. Note that technical editing may introduce minor changes to the manuscript text and/or graphics which could affect content, and all legal disclaimers and ethical guidelines that apply to the journal pertain. ACS cannot be held responsible for errors or consequences arising from the use of information contained in these “Just Accepted” manuscripts.

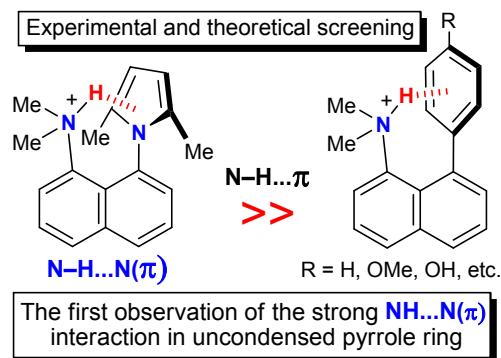
# Modeling Biologically Important NH... $\pi$ Interactions Using *peri*-Disubstituted Naphthalenes

Alexander F. Pozharskii,<sup>\*a</sup> Olga V. Dyablo,<sup>a</sup> Olga G. Pogosova,<sup>a</sup> Valery A. Ozeryanskii,<sup>a</sup> Aleksander Filarowski,<sup>b</sup> Kseniya M. Vasilikhina,<sup>a</sup> Narek A. Dzhangiryan<sup>a</sup>

<sup>a</sup> Department of Organic Chemistry, Southern Federal University, Zorge 7, 344090 Rostov-on-Don, Russian Federation

<sup>b</sup> Faculty of Chemistry, University of Wrocław, F. Joliot-Curie 14, 50-383 Wrocław, Poland

Corresponding author. E-mail address: [apozharskii@sfedu.ru](mailto:apozharskii@sfedu.ru)



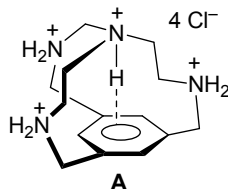
**Abstract.** For the first time, systematic studies of 8-aryl and 8-pyrrolyl derivatives of 1-aminonaphthalene as simple, synthetically available and nicely preorganized models were conducted for a better understanding the properties of NH... $\pi$  interactions involved in the stabilization of the secondary and tertiary protein structures as well as the recognition of guest molecules by biological receptors. It was shown that the NH... $\pi$  binding is especially effective when the NH-donor is a positively charged group, e.g.  $\text{Me}_2\text{NH}^+$ , and the  $\pi$ -donor is an electron-rich aromatic substituent, in particular, 1-pyrrolyl or 4-hydroxyphenyl groups. Using protonated tetrafluoroborate salts, a strong counterion effect was demonstrated by means of theoretical calculations. Through several mechanisms, including short CH...F contacts, bifurcation and long-range dispersion, the counterion promotes considerable structural changes and weakening the NH... $\pi$  interactions from 12–15 kcal mol<sup>-1</sup> in “naked” cations to 5–9 kcal mol<sup>-1</sup> in the salts. To this end, 8-(2,5-dimethylpyrrol-1-yl)-*N,N*-dimethylnaphthalene-1-ammonium tetrafluoroborate, with the record linearity and shortness (2.07 Å) of the NH... $\pi$ -centroid bond, was recognized as the most appropriate model with the strongest NH... $\pi$  interaction ever described.

## Introduction

According to Pauling’s discovery, made in the middle of the last century, the secondary structure of majority of natural proteins represents the so-called right-handed  $\alpha$ -helix.<sup>1</sup> It is maintained inside each of its coils mainly by the amide NH...O=C hydrogen bonds (HB). However, after some time, evidences began to appear that other forms of noncovalent interactions, in particular, the salt ones, as

well as OH... $\pi$  and NH... $\pi$ , are involved in the formation of the secondary and tertiary (crumpled spiral form) structures.<sup>2</sup> Three proteinogenic amino acids containing aromatic nuclei, namely phenylalanine, tyrosine and tryptophan, play the role of the proton acceptor in the XH... $\pi$  hydrogen bonds. It was also established that, in addition to the stabilization of the protein structure, XH... $\pi$  interactions are responsible for the recognition of drugs<sup>2e</sup> and other biologically important molecules within the “host-guest” and receptor chemistry concepts.<sup>2f,g</sup> The study of  $\pi$ -interactions on real objects is rather complicated for various reasons and therefore it is more convenient to simulate them on simpler synthetic models.<sup>2a</sup> To date, a lot of efforts have been made in this direction. Most of them are associated with supramolecular caged ligands like calixarenes, cryptands, podands, metal complexes, etc.<sup>2f,3,4</sup> In them, aromatic nuclei and proton donor groups are normally fixed (preorganized) for effective XH... $\pi$  interaction. Given the prevalence of neutral and charged amino groups in proteins, we were especially interested in modeling NH... $\pi$  interactions. According to current databases over the past quarter century, about two dozen reports related to this topic have appeared. Their analysis reveals the main trends of this approach, as well as its advantages and disadvantages. Primarily, it is not easy to arrange the internal cavity and receptor part of the caged ligands in such a way that it would be ideally suited for a particular guest molecule. The cavity may be too narrow or, conversely, have large voids. In the first case, NH... $\pi$  interaction often proceeds from the outside and is loose and vulnerable to external influences, in particular to solvation effects. Indeed, in most of the articles cited, the  $\pi$ -donor component, benzene as a rule, interacted with the NH receptor from the outside of the host molecule (ESI, Table S1).<sup>3a-f</sup> Rarely, the NH component acted as an external guest molecule.<sup>3g-i</sup> There are quite a few examples of the effective NH... $\pi$  interaction inside the molecular framework.<sup>2f,4</sup> It is not surprising that such a variety of situations results in a large spread in the parameters of the NH... $\pi$  bond. For example, the distance from the NH proton to the benzene ring centroid (this point is designated in this work as M) covers the range of 2.17–2.98 Å. Another drawback of this approach is a rather difficult synthesis of frame structures, often bearing multiple functional groups, that complicates some studies, especially in solution. Thus, almost in all the cited publications no information is presented concerning chemical shifts of the NH proton engaged in the NH... $\pi$  binding. This can be illustrated by one of the best works of this kind, performed by Steed’s group.<sup>4a</sup> They synthesized the small tetraazaphane **A**, in the inner cavity of which only a proton, but not other Lewis acids, could be placed. However, selective monoprotection of the bridging nitrogen atom was not possible, since the external nitrogens were first protonated. Ultimately, the authors have obtained only tetrahydrochloride, XRD analysis of which showed the perfect orientation of the internal N–H bond to the benzene centroid with a very short

NH...M distance of 2.17 Å. Regrettably, in solution no signal of the internal NH proton could be detected due to its fast exchange with the external protons.



In order to improve the above situation, for studying NH... $\pi$  interactions in the present work we chose *peri*-disubstituted naphthalenes **1–8** as simpler and easily accessible models (Figure 1). Another important advantage of these compounds is the presence of the “proximity effect”<sup>5</sup> between proton-donor and proton-acceptor fragments, which provides the necessary preorganization of the interacting sites combining with their optimal flexibility. As the proton-acceptors ( $\pi$ -donors), phenyl, *p*-anisyl, *p*-hydroxyphenyl, 2-naphthyl, pyrrol-1-yl and 2,5-dimethylpyrrol-1-yl groups were selected. The protonated NMe<sub>2</sub> group along with NH-pyridinium cation (see also compound **31**) and neutral amino and acetamido groups served as proton donors.<sup>6</sup> The choice of these proton donors is explained by a wide range of their NH-acidity ( $pK_a \approx 5$ –27), as well as their abundance in living tissues. It should be noted that the results of the study of salt **1** and its analogue with the unsubstituted pyrrolyl group instead of the phenyl one were reported by us in a slightly different context in recent articles.<sup>7,8</sup>

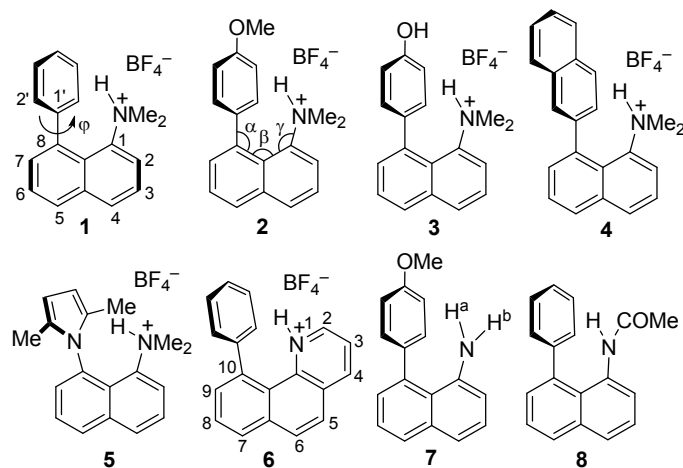


**Figure 1.** Compounds for which NH... $\pi$  interactions were studied.

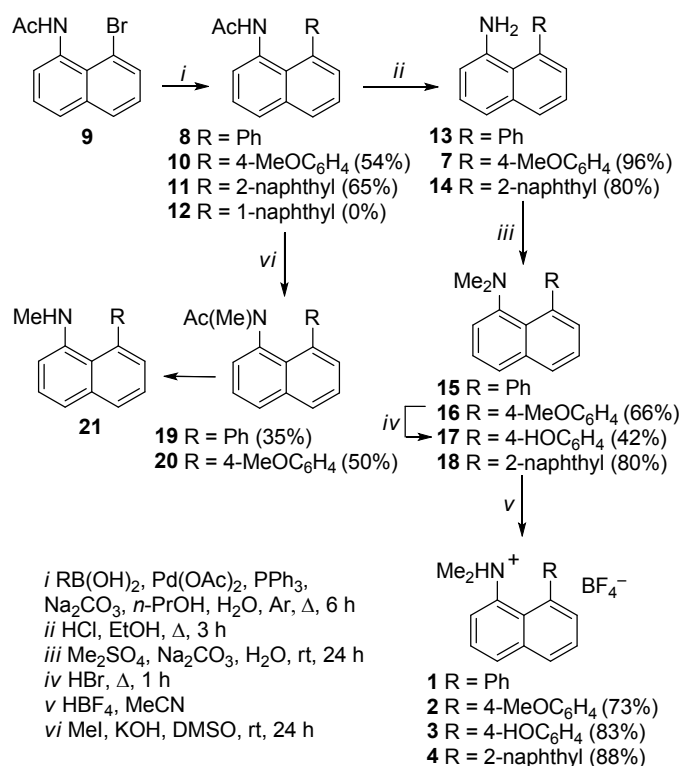
The main methods for studying the NH... $\pi$  hydrogen bonds in this work were XRD measurements for the solid state, <sup>1</sup>H NMR and IR spectroscopy for solutions and quantum-chemical calculations for MeCN solution and the gas phase.

## Results and discussion

### Synthesis

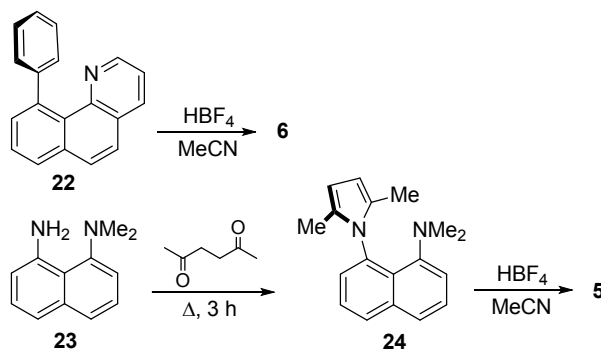
The synthetic approaches to compounds **1–4**, as well as **7** and **8**, are shown in Scheme 1. In most cases, the starting material was 1-bromo-8-acetamidonaphthalene **9**,<sup>9</sup> which was subjected into the Suzuki reaction to introduce an aryl substituent with the following deacetylation and exhaustive methylation of the amino group. It should be noted that the reaction of **9** with naphthyl-1-boronic acid, to obtain compound **12**, could not be carried out under a wide range of conditions. However, the same reaction with naphthyl-2-boronic acid proceeded without complications, leading to compounds **11**, **14** and **18** in good yields. Phenol **17** was obtained by demethylation of 4-methoxyphenyl derivative **16** with hydrobromic acid. Initially, we also intended to study the salts of monomethyl derivatives **21**. For this, by methylation of the acetamido group in compounds **8** and **10**, we obtained compounds **19**, **20**. However, all attempts to carry out their deacetylation failed; the difficulties of carrying out such reactions for some other *peri*-substituted naphthalenes were reported previously.<sup>10</sup>

**Scheme 1.** Synthesis of Compounds **1–4**, **7** and **8**



10-Phenylbenzo[*h*]quinoline (**22**) used to generate salt **6** was prepared by direct phenylation of benzo[*h*]quinoline as described earlier<sup>11</sup> while for the preparation of 1-(2,5-dimethylpyrrol-1-yl)-8-dimethylaminonaphthalene (**24**) the interaction of *peri*-diamine **23** with 2,5-hexanedione was employed (Scheme 2). The target salts **1–6** were obtained on addition of equimolar amount of aqueous tetrafluoroboric acid to a solution of the corresponding base in acetonitrile or ethyl acetate.

## Scheme 2. Preparation of Protonated Models 5 and 6



## Solid State Structures

As the main parameters indicating the formation and peculiarities of the NH... $\pi$  hydrogen bonding in the crystalline state of the studied substances, we considered the NH...M and NH...C1 distances, the NHM angle, the rotation angle of the aryl (pyrrolyl) substituent relative to the naphthalene ring and the HNC1C2 torsion angle, showing the directionality of the NH bond to the plane of the aromatic  $\pi$ -system. In addition, we were interested in the degree of deformation of the naphthalene ring, in particular, the so-called “twisting”  $\Theta$  (torsion angle between the C2–C3/C6–C7 bonds which are highlighted in structure 1 in bold lines) and the angles  $\alpha$ ,  $\beta$  and  $\gamma$  (see structure 2). It should be noted that the distortions of the naphthalene ring as a whole turned out to be small and little variable; therefore less attention was paid to them. At the same time, for salts 1–6, useful information was obtained from the minimum distances between the chelated NH proton and the nearest fluorine atom in the counterion, NH...F $B_3^-$ . All this and a number of other information are depicted in Table 1 and in Figures 2, 4–6.

**Table 1.** Selected Bond Lengths, Distances (Å) and Angles (°) for Compounds 1–8

(with indicated uncertainties; all XRD measurements were performed at 120 K except 100 K for salt 4)

Parameter	Compound							
	1	2	3 <sup>a</sup>	4	5	6	7	8
$\varphi^b$	83.8 (84.1)	78.7 (76.4)	86.1 (84.3)	73.5 (70.3)	88.1 (86.9)	62.8 (57.4)	76.1 (74.3)	48.5 (45.1)
$\angle$ HNC1C2	178(2)	171(2)	178(4)	177(2)	174(2)	177(2) <sup>c</sup>	145(6) <sup>d</sup> 167(4) <sup>e</sup>	60(4)
N–H	0.91(2)	0.89(2)	0.91(3)	0.89(4)	0.90(2)	0.90(2)	0.85(7) <sup>d</sup> 1.07(4) <sup>e</sup>	0.87(2)
NH...M <sup>f</sup>	2.39(2)	2.41(2)	2.45(3)	2.56(4)	2.07(2)	2.84(2)	2.70(4) <sup>d</sup>	3.66(2)
$\angle$ NHM <sup>f</sup>	173(2)	165(2)	172(3)	167(3)	171(2)	153(2)	144(5) <sup>d</sup> 126(4) <sup>e</sup>	75(2)
NH...C1'	2.06(2)	2.06(2)	2.05(3)	2.08(4)	2.07(2)	2.29(2)	2.30(4)	2.84(2)

$\angle\text{NHC1}^g$	146(2)	148(2)	151(4)	147(3)	144.1(11)	118.1(12)	125(4)	118.2(11)
$\Theta^h$	0.6(3)	1.3(3)	1.0(4)	2.8(3)	0.5(2)	3.7(2)	1.4(4)	11.8(2)
$\alpha, \beta, \gamma^i$	123.0(2)	123.2(2)	124.0(2)	124.4(2)	120.97(12)	125.95(12)	124.4(2)	124.1(2)
	127.0(2)	127.2(2)	126.8(2)	126.1(3)	127.36(12)	125.74(12)	125.3(2)	125.8(2)
	121.0(2)	120.6(2)	120.9(2)	120.0(2)	121.99(13)	122.60(12)	122.7(2)	122.3(2)
$\text{NH}\dots\text{FBF}_3^-$	3.67(2)	3.55(2)	3.30(3) <sup>j</sup>	3.14(4)	4.21(2)	2.19(2)	–	–

<sup>a</sup> Average values for 4 independent cations; <sup>b</sup> Rotation angle of the aryl (pyrrolyl) substituent relatively the average naphthalene ring plane. Estimation of the same parameter via torsion angle C7C8C1'C2' is given in brackets. <sup>c</sup> Torsion angle HNC1aC4a (atom numbering corresponds to the IUPAC rules). <sup>d</sup> For H<sup>a</sup> atom of NH<sub>2</sub> group (see Figure 1). <sup>e</sup> For H<sup>b</sup> atom of NH<sub>2</sub> group. <sup>f</sup> M – centroid of the phenyl (pyrrolyl) substituent; in case of **4**, the M refers to the lower benzene ring. <sup>g</sup> NHC2 and NHN for compounds **4** and **5**, respectively. <sup>h</sup> Torsion angle C2–C3/C6–C7. <sup>i</sup> The values of these angles are given from top to bottom, respectively. <sup>j</sup> Average value for two of four independent molecules; two others form dimer pairs due to NH...OH binding, in which the BF<sub>4</sub><sup>-</sup> counterions are located outside the cations at the NH...FBF<sub>3</sub><sup>-</sup> distances of 4.37(3) and 4.95(3) Å.

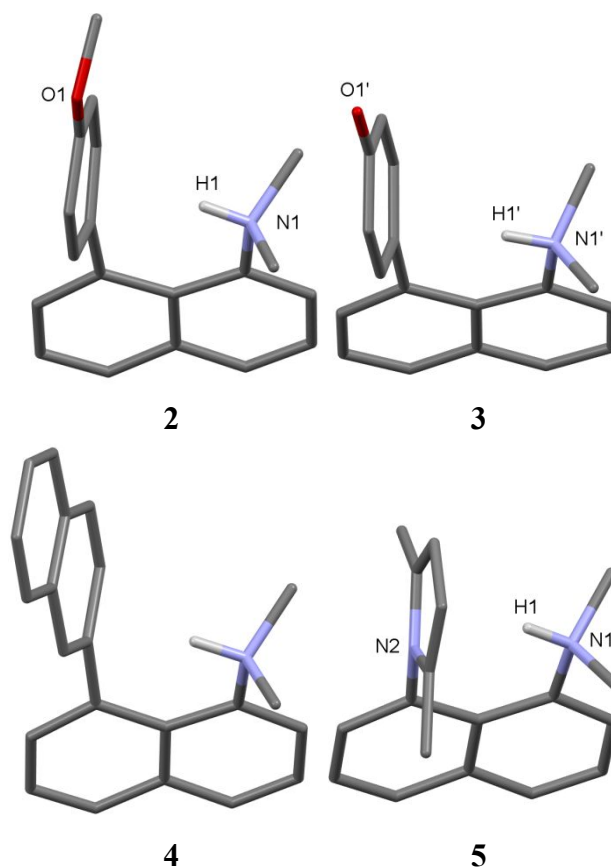


**Figure 2.** Representative solid state molecular structures of compounds **2–5** showing general arrangement of the *peri*-substituents directed to the viewer (capped stick models, hydrogen atoms, except the NH proton, and BF<sub>4</sub><sup>-</sup> anions are omitted for clarity).

Obviously, the main sign of the NH... $\pi$  interaction is the strict orientation of the N–H bond onto the aromatic ring face. Ideally, this should be manifested in the rotation of the latter relative to the naphthalene ring plane by angle  $\varphi = 90^\circ$  (see structure **1** in Figure 1). At the same time, the N–H bond should lie in the plane of the naphthalene system or close to it, which can be expressed through the

torsion angle HNC1C2 or alternatively through the angle between the planes of the naphthalene ring and HNC1.

According to the Cambridge Structural Database (CCDC), aromatic nuclei in the solid diphenyl and 2,2'-binaphthyl are coplanar ( $\varphi = 0^\circ$ ). In contrast, in 1,1'-binaphthyl  $\varphi = 68.5^\circ$  while information on 1,2'-binaphthyl, 1-phenyl-, 1-*p*-anisyl-, 1-*p*-hydroxyphenyl- and 1-(pyrrol-1-yl) naphthalenes in the CCDC is absent. There is little doubt that in the last five compounds the bi-nuclear systems should be noncoplanar due to *peri*-interaction with the proton in position 8. Therefore, it seems logical to count the rotation angle  $\varphi$  of the aryl substituent in compounds **1–5** not from the hypothetical planar structure with  $\varphi = 0^\circ$ , but from the value of  $\varphi$  in compounds **25–29**. In this case, the corresponding difference,  $\Delta\varphi$ , should better reflect the stimulus of the aromatic substituent to the NH... $\pi$  interaction. Following these considerations, we performed a DFT calculation of the angle  $\varphi$  in molecules **25–29** for the gas phase, and for the first three substances also for the solution in acetonitrile. The B3LYP/6-311++G\*\* level of theory was used, since previously for proton sponges it gave good agreement between theoretically calculated and experimental structural characteristics.<sup>12</sup> The obtained  $\varphi$  values are shown in Figure 3.

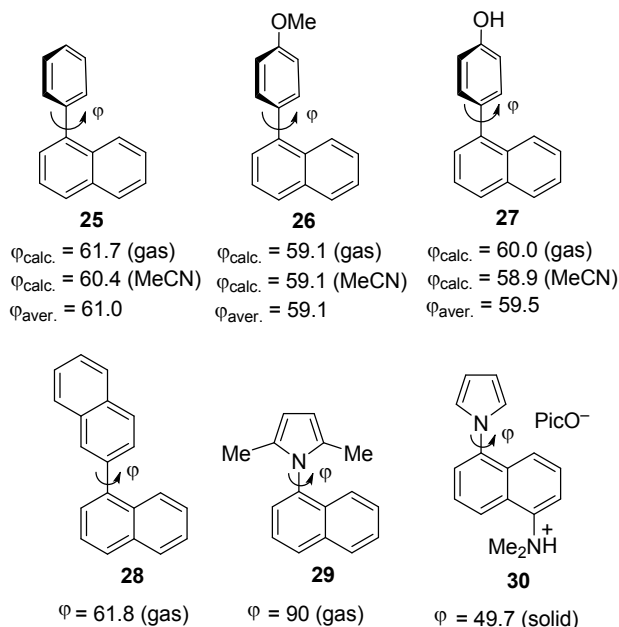
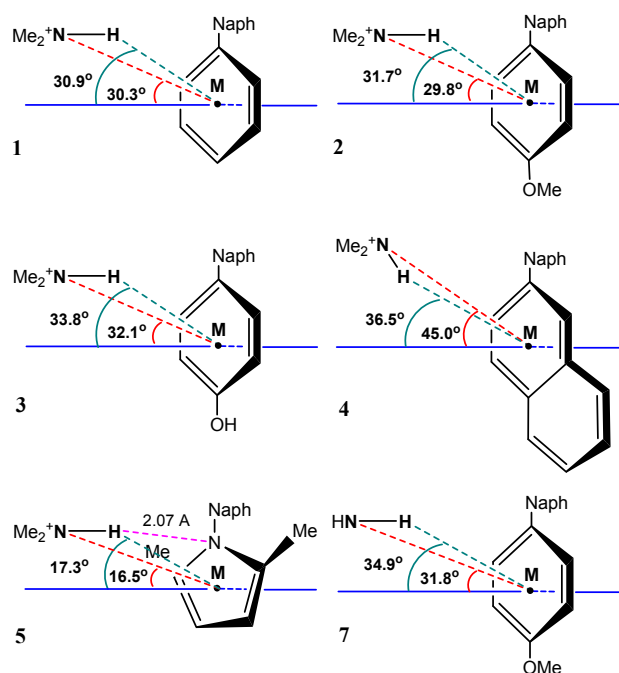


**Figure 3.** Compounds used for estimation of rotation angle  $\varphi$  ( $^\circ$ ) when NH... $\pi$  interactions are absent (theoretically calculated values for **25–29**, XRD data for **30**, see ref. 7).

As can be seen, the  $\varphi$  values for compounds **25–27** differ little for the gas phase and the solution. Therefore, when evaluating the parameter  $\Delta\varphi$  for them, we were guided by the average values of the calculated rotation angle  $\varphi_{\text{aver.}}$ . Only in the case of dimethylpyrrolynaphthalene **29** both nuclei are

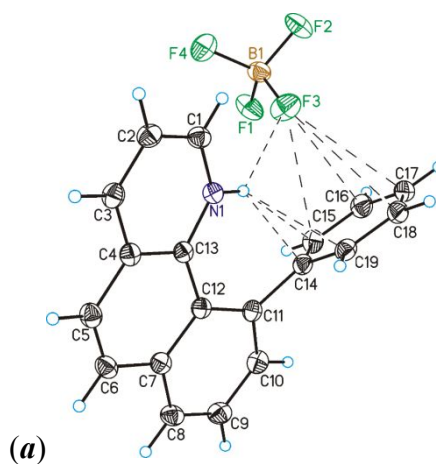
perfectly orthogonal, which reflects the strong steric repulsion of the  $\alpha$ -methyl groups and the H-8/H-2 protons. A weighty argument in favor of such repulsion is the fact that in 1-pyrrolynaphthalene **30**, for which XRD data are available, the angle  $\varphi$  is only near  $50^\circ$  (see also ESI, p. S28).<sup>7</sup> Clearly, a sharp difference between the latter value and  $90^\circ$ , like between  $\varphi$  for **25–28** and  $90^\circ$ , reflects a compromise among the steric repulsion of the two nuclei and their tendency to conjugate with each other.

The obtained  $\Delta\varphi$  values, which, we believe, result from the tendency of the aryl nuclei to participate in the NH... $\pi$  interaction, for compounds **1–4** are 22.8, 19.6, 26.6, and  $11.7^\circ$ , respectively. As for compound **5**, it is preorganized for the NH... $\pi$  interaction with the *peri*-HN<sup>+</sup>Me<sub>2</sub> group from the very beginning. Nevertheless, it seemed yet interesting to apply the above approach to **5** assuming that, by analogy with **30** the angle of rotation  $\varphi$  in reference compound **29** is also close to  $50^\circ$ . A purely hypothetical value of  $\Delta\varphi$  for **5** estimated by this way is  $\sim 38^\circ$ . Thus, in any case, the 2,5-dimethyl-1-pyrrolyl group, followed by the *p*-hydroxyphenyl, phenyl, *p*-anisyl and 2-naphthyl groups, manifests the largest degree of NH... $\pi$  interaction in the solid tetrafluoroborates **1–5**. Common in biochemical practice,<sup>2c</sup> the analysis of the N–H...M hydrogen bond linearity, estimated via the angle between the normal to the aromatic centroid and the N–H bond, leads to a close conclusion (Figure 4). As can be seen, for compound **5** ( $17^\circ$ ) the HB linearity is half as much as for **1–4** ( $31–37^\circ$ ). Apparently this geometrical circumstance along with the higher  $\pi$ -donating ability of the pyrrolyl group in **5** recalls with the relative contribution of tryptophan, tyrosine and phenylalanine in stabilisation of protein structures changing in proportion 5 : 1.5 : 1.<sup>2c</sup>



**Figure 4.** Schematic illustration of relative NH... $\pi$  hydrogen bond linearity in compounds **1–5** and **7**.

1  
2 Important structural feature of salts **1–5** is that the NH proton in their cations is hidden into a tight  
3 hydrophobic pocket formed, on the one side, by an aryl group (a kind of specific wall), and by the  
4 NMe<sub>2</sub> group on the other side. In the case of **5** the NH proton is additionally shielded by the *ortho*-  
5 methyl groups of the pyrrole ring. This is supported by the values of the shortest distances between the  
6 chelated NH proton and the BF<sub>4</sub><sup>-</sup> anion. Those noticeably exceed 3 Å what should prevent the NH... $\pi$   
7 hydrogen bond from bifurcation and therefore from distortion (Table 1). For comparison, in the  
8 tetrafluoroborate of protonated 1,8-bis(dimethylamino)naphthalene (proton sponge), the NH...F  
9 distance is 2.91 Å, while in the tetrafluoroborates of such compounds as 2,2'-dipyridyl and *o*-  
10 phenanthroline, called pseudo-proton sponges,<sup>13</sup> the NH...F contact falls down to 1.9–2.3 Å and the  
11 intramolecular HB in them becomes strongly bifurcated. The tetrafluoroborate of 10-  
12 phenylbenzo[*h*]quinolinium **6**, for which the NH...F distance is 2.19 Å, definitely also belongs to this  
13 class of compounds. Since there is no steric shielding of the NH proton in **6**, the BF<sub>4</sub><sup>-</sup> anion is able to  
14 approach it closer and enter into the bifurcation interaction. This causes a considerable weakening of  
15 IHB in **6** what is clearly seen in Figure 5a and the corresponding parameters given in Table 1. For the  
16 same reason, two NH... $\pi$  hydrogen bonds in the structurally related bis(tetrafluoroborate) **31** are even  
17 more weakened (Figure 5b). Indeed, the NH...M distances in **31** are near 3.1 Å versus 2.8 Å for its  
18 monomeric analogue **6** and 2.4 Å for salts **1–4**, not to mention salt **5** (2.1 Å). Note that the base of  
19 10,10'-dibenzo[*h*]quinoline was described previously<sup>14a</sup> but its bis(tetrafluoroborate) was obtained and  
20 studied by us for the first time.<sup>14b</sup>



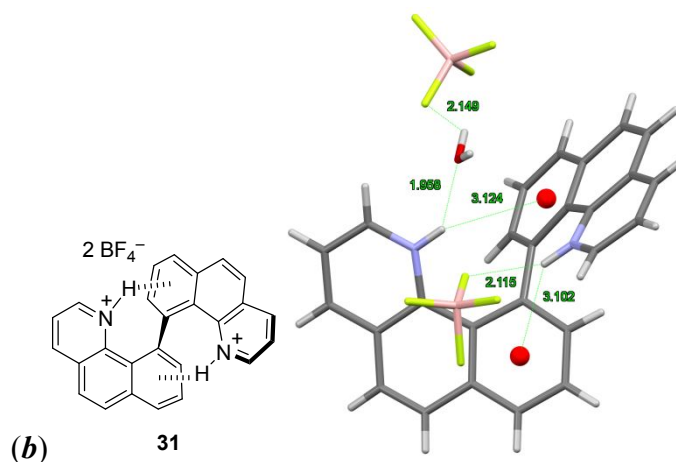


**Figure 5.** Molecular structures of (a) salt **6** ( $P = 50\%$ , short contacts between the interacting atoms are shown by dashed lines) and (b) bis(tetrafluoroborate) of 10,10'-dibenzo[*h*]quinolinium monohydrate (**31**) (with indication of short contacts around both the NH protons).

Although the non-protonated forms of salts **1–6** are still not structurally characterized (mainly due to the fact that bases **15–18** and **22** are liquid at room temperature or fusible as **24**), the contraction of the N...M distance upon protonation might serve as another measure of NH... $\pi$  binding. There is a single example when such estimation can be done. Thus, when going from neutral 1-dimethylamino-8-(pyrrolyl-1)naphthalene<sup>7</sup> to salt **5** (here, however, two C–Me groups are added, but they have little effect on the pyrrole cycle geometry), the distance to the pyrrole centroid N...M decreases from 3.354 to 2.960 Å, that is by 12%, and the repulsive interaction of *peri*-substituents becomes attractive. In general, taking into account the smallest angle  $\alpha$  ( $\alpha = 120.97^\circ$ , Table 1) and the striking equality<sup>15</sup> of the NH...M and NH...N distances (both 2.07 Å) in **5**, the NH... $\pi$  interaction in this salt should be considered the strongest in this and related series. Simultaneously, this is the first observation of the NH...N( $\pi$ ) interaction in uncondensed pyrrole ring.

We now turn to compound **7**, which contains a neutral amino group with the substantially less acidic N–H bonds than in salts **1–6**. The first thing that attracts attention in the structure of **7** (Figure 6) is a considerable pyramidalization of the nitrogen atom ( $\Sigma N = 338.3^\circ$ ) sharply contrasting with the completely flat and coplanar with the ring NH<sub>2</sub> group in 1-aminonaphthalene ( $\Sigma N = 360.0^\circ$ ).<sup>16</sup> The second peculiarity of the amino group in **7** is the notable shortening of the N–H bond facing the *p*-anisyl substituent (0.85 Å) if compared with the external N–H bond (1.07 Å). Apparently, this may be due to a small interpenetration of the van der Waals spheres of the benzene ring and the internal NH<sub>2</sub> hydrogen atom, what breaks the planarity and symmetry of the NH<sub>2</sub> group. Indeed, the van der Waals radius of the hydrogen atom is 1.20 Å, and the half-width of the benzene ring is 1.70 Å.<sup>17</sup> Their sum (2.90 Å) somewhat exceeds the NH...M distance (2.70 Å) in amine **7**. At the same time, in salts **1–5**,

the NH...M contacts are markedly shorter (2.07–2.45 Å), meaning much stronger interpenetration of the electron shells of the NH proton and the benzene (pyrrole) ring. With such characteristics, the NH... $\pi$  hydrogen bond in salts **1–5** should have a significant covalent component unlike **7** in which the hydrogen bond is considerably weaker due to predominantly electrostatic nature. Additional signs of this are a reduced rotation angle ( $\Delta\phi = 17^\circ$ ) of the *p*-anisyl group in **7** relative to reference compound **26**, as well as a slightly lower linearity of the hydrogen bond than in salts **1–3** and **5** (Figure 4).

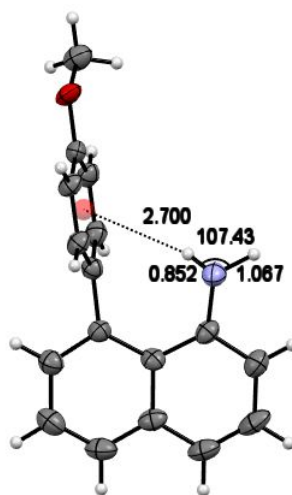


**Figure 6.** Molecular structure of amine **7** with the indication of key parameters ( $P = 50\%$ ).

Given the higher NH-acidity of carboxamides ( $pK_a \sim 14\text{--}15$ ) compared with arylamines ( $pK_a \sim 27$ ),<sup>18</sup> we assumed that the NH... $\pi$  binding would also be possible in compound **8**. However, XRD measurements showed that crystal lattice of **8** is formed exclusively by the intermolecular amide bonds NH...O=C (ESI, Figure S42).

### Solution Structures

Based on the classical example of the CH... $\pi$  hydrogen bond between chloroform and benzene, which manifests itself in notable shielding ( $\Delta\delta_{CH} = -1.56$  ppm)<sup>19</sup> of the CHCl<sub>3</sub> proton (Figure 7, structure **32**),<sup>20,21</sup> we reasoned that a similar effect can be used to estimate the NH... $\pi$  chelation in the compounds under study. The corresponding data on the chemical shifts,  $\delta_{NH}$ , and the paramagnetic shift,  $\Delta\delta_{NH}$ , relative to a reference compound not bearing an aromatic substituent in the adjacent *peri*-position are depicted in Table 2. As reference compounds there were taken 1-aminonaphthalene **33**, 1-acetamidonaphthalene **34** and tetrafluoroborates of dimethyl(naphth-1-yl)ammonium **35** and benzo[*h*]quinolinium **36** (Figure 7). Acetonitrile served as a solvent for salts of types **B** and **C**, and chloroform for neutral amines **D** and carboxamides **E**.

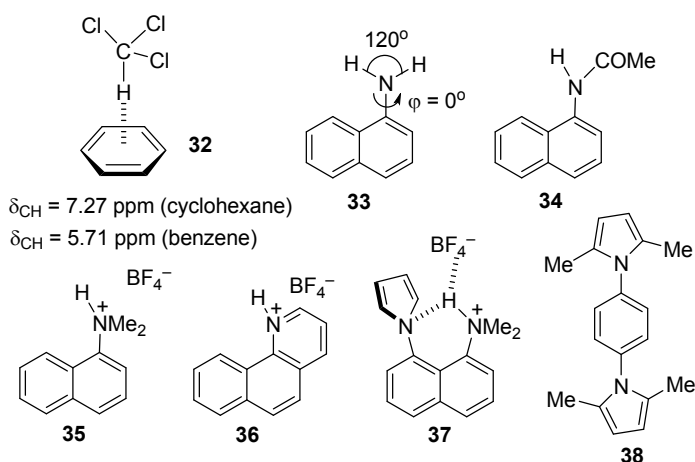
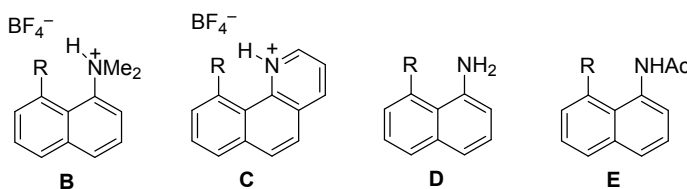


**Figure 7.** Auxiliary compounds and interacting systems used in the discussion.

**Table 2.** Changes in the NH Proton Chemical Shifts in Compounds **B–E** Induced by Paramagnetic Component of Ring Current of Aryl and Pyrrolyl Groups



Type of compd.	R	No	Solvent	$\delta_{\text{NH}}$ , ppm	$\Delta\delta_{\text{NH}}$ , ppm	Ref.
<b>B</b>	H	<b>35</b>	CD <sub>3</sub> CN	9.47	–	<i>a</i>
<b>B</b>	Ph	<b>1</b>	CD <sub>3</sub> CN	8.09	–1.38	<i>b</i>
<b>B</b>	4-MeOC <sub>6</sub> H <sub>4</sub>	<b>2</b>	CD <sub>3</sub> CN	8.45	–1.02	<i>a</i>
<b>B</b>	4-HOC <sub>6</sub> H <sub>4</sub>	<b>3</b>	CD <sub>3</sub> CN	8.57	–0.90	<i>a</i>
<b>B</b>	naphth-2-yl	<b>4</b>	CD <sub>3</sub> CN	8.30	–1.17	<i>a</i>
<b>B</b>	2,5-dimethyl-pyrrol-1-yl	<b>5</b>	CD <sub>3</sub> CN	6.20	–3.27	<i>a</i>
<b>B</b>	pyrrol-1-yl	<b>37</b>	CD <sub>3</sub> CN	6.40	–3.07	<i>c</i>
<b>C</b>	H	<b>36</b>	CD <sub>3</sub> CN	13.92	–	<i>a</i>
<b>C</b>	Ph	<b>6</b>	CD <sub>3</sub> CN	12.35	–1.57	<i>a</i>
<b>C</b>		<b>31</b>	CD <sub>3</sub> CN	12.50	–1.42	<i>a</i>
<b>D</b>	H	<b>32</b>	CDCl <sub>3</sub>	4.04	–	<i>d</i>
<b>D</b>	Ph	<b>13</b>	CDCl <sub>3</sub>	3.72	–0.32	<i>a</i>
<b>D</b>	4-MeOC <sub>6</sub> H <sub>4</sub>	<b>7</b>	CDCl <sub>3</sub>	3.69	–0.35	<i>a</i>
<b>D</b>	naphth-2-yl	<b>14</b>	CDCl <sub>3</sub>	3.70	–0.34	<i>a</i>
<b>E</b>	H	<b>34</b>	CDCl <sub>3</sub>	7.96	–	<i>a</i>
<b>E</b>	Ph	<b>8</b>	CDCl <sub>3</sub>	7.03	–0.93	<i>e</i>
<b>E</b>	4-MeOC <sub>6</sub> H <sub>4</sub>	<b>10</b>	CDCl <sub>3</sub>	7.19	–0.77	<i>a</i>
<b>E</b>	naphth-2-yl	<b>11</b>	CDCl <sub>3</sub>	6.97	–0.99	<i>a</i>

*a* This work. *b* Ref. 7. *c* Ref. 8. *d* Spectral database of organic compounds (SDBS № 1171); Internet resource: ([http://sdbs.db.aist.go.jp/sdbs/cgi-bin/cre\\_index.cgi](http://sdbs.db.aist.go.jp/sdbs/cgi-bin/cre_index.cgi)). *e* Ref. 9.

From Table 2 it follows that the largest paramagnetic shifts,  $\Delta\delta_{\text{NH}}$ , are observed for salts **5** and **37** with 1-pyrrolyl group, 3.27 and 3.07 ppm respectively, whereas for their aryl analogues **1–4** such values are 2.5–3 times less (0.90–1.38 ppm), and for neutral amine **7** even 0.35 ppm. It seemed reasonable to assume that there could be some correlation between the magnitudes of  $\Delta\delta_{\text{NH}}$  and the NH...M distances. To test this idea we built the corresponding plot for cations **1–6**, **31**, **37** having the charge-assisted NH... $\pi$  hydrogen bonds and included in it also amine **7** (Figure 8). As expected, the points for benzo[*h*]quinolinium cations **6** and **31** and amine **7** (red circles) strongly dropped out of the graph, apparently due to the bifurcation of IHB in two first salts and the absence of IHB in solution of **7** (see below). At the same time, the observed linear relationship for cations **1–5** and **37** is quite satisfactory with the correlation coefficient  $R^2 = 0.9682$ . Interestingly, that a certain correlation with  $R^2 = 0.9535$  exists for all salts, including **6** and **31**, when using the chemical shift values,  $\delta_{\text{NH}}$ , instead of the  $\Delta\delta_{\text{NH}}$  parameter (ESI, Figure S43).

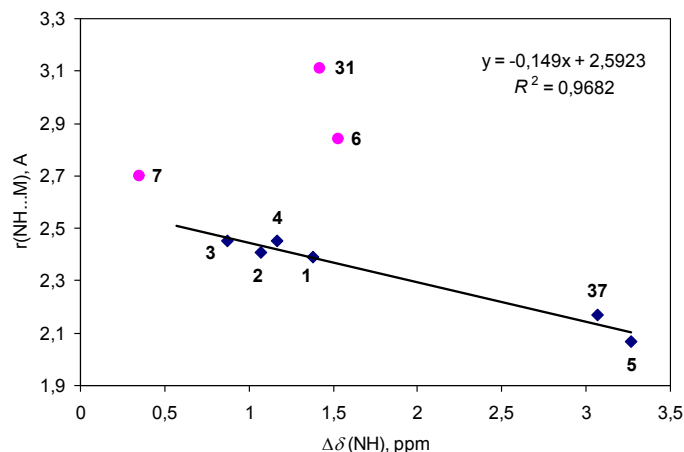


**Figure 8.** Correlation of the  $\Delta\delta(\text{NH})$  values versus the XRD NH...M distances for the tetrafluoroborates **1–5** and **37**. Since for pyrrole derivative **37** diffraction measurements could not be performed (ref. 8) the DFT gas-phase distance was used in this case.

As for amine **7**, all the data indicate that, unlike the solid state, the intramolecular NH... $\pi$  binding is absent in its solutions. Indeed, in the  $^1\text{H}$  NMR spectrum of **7** in  $\text{CDCl}_3$ , the NH protons give a one two-proton signal at  $\delta$  3.69 ppm. Their equivalence is maintained upon cooling to  $-90$  °C, indicating the low barrier rotation of the amino group in the given temperature range (ESI, Figure S4). An insignificant paramagnetic shift of the  $\text{NH}_2$  signal relative to 1-aminonaphthalene ( $\Delta\delta_{\text{NH}} = -0.35$  ppm) as well as in spectra of amines **13** and **14** can be a reflection of both different hybridization of the nitrogen atoms in **33** and **7**, and a short-term alternate staying of each NH proton in the paramagnetic field of the adjacent aromatic ring. The absence of a stable NH... $\pi$  hydrogen bond in **7** is also confirmed by IR spectroscopy. Indeed, the bands of symmetric and antisymmetric stretching vibrations

of the NH<sub>2</sub> group in a solution of **7** in CCl<sub>4</sub> ( $\nu_s = 3401$ ;  $\nu_{as} = 3495$  cm<sup>-1</sup>) as compared with amine **33** ( $\nu_s = 3395$ ;  $\nu_{as} = 3476$  cm<sup>-1</sup>) are moved not to the red region as normally occurs at the hydrogen bonding (including NH... $\pi$  one), but to the blue one (ESI, Table S2, Figures S44 and S45).<sup>22</sup>

The situation for carboxamides **8**, **10** and **11** looks ambiguously. In their <sup>1</sup>H NMR spectra in CDCl<sub>3</sub> a relatively small paramagnetic shift is observed for NH proton ( $\Delta\delta_{\text{NH}} = -0.77\dots-0.99$  ppm) as compared with 1-acetamidonaphthalene **34** (Table 2). At the same time, in the IR spectra of **8** and **10**, the  $\nu_{\text{NH}}$  band undergoes a strong shift to the high-frequency region of the spectrum (Table 3). In our opinion, the IR data, indicating the absence of NH... $\pi$  interaction in amides **8** and **10**, are more reliable. The blue shift of the  $\nu_{\text{NH}}$  band, as well as increase of the  $\nu_{\text{CO}}$  frequency and the paramagnetic shift of the NH signal in <sup>1</sup>H NMR spectra can be interpreted as a result of the destruction of the carboxamide associates (see ESI, Figure S42).

**Table 3.** IR Spectra of 1-Acetamido-8-arylnaphthalenes (NH and C=O groups region, 0.1 M solutions in CCl<sub>4</sub>)

Compd.	$\nu_{\text{NH}}$ , cm <sup>-1</sup>	$\nu_{\text{CO}}$ , cm <sup>-1</sup>	$\Delta\nu_{\text{NH}}$ , cm <sup>-1</sup>	$\Delta\nu_{\text{CO}}$ , cm <sup>-1</sup>
<b>8</b>	3426	1701	+157	+50
<b>10</b>	3437	1704	+169	+53
<b>34</b>	3269	1651	–	–

### NH... $\pi$ Bond Energy

Finally, we wished to estimate, at least roughly, the energy of NH... $\pi$  interactions in the compounds studied. For this, salts **1–3** and **5** were selected. It should be emphasized that there are still no reliable experimental methods for estimating the energy of intramolecular noncovalent interactions. What concerns theoretical approaches they also differ by insufficient accuracy and various limitations. For example, we have recently shown<sup>7</sup> that the so-called “isodesmic” calculation method<sup>23</sup> does not work in the case of salts of type **1–5**, and in the present work, the NBO (natural bond orbital) method<sup>24</sup> also failed. In this regard, we focused on the “rotational” approach,<sup>7,25</sup> according to which the  $E_{\text{HB}}$  energy is defined as a difference between the total energies of two optimized structures, the close (chelated) and open (non-chelated) one (Figure 9). To achieve the goal, we performed the DFT calculations of the IHB energies,  $E_{\text{HB}}$ , using the B3LYP method with the 6-311++G(d,p) basis set. The calculations were conducted for the gas phase and acetonitrile solution. Besides, we also performed calculation of  $E_{\text{HB}}$  values using the Grimme's D3 dispersion correction.<sup>26</sup> It comes from an idea that quantification of intramolecular phenomena can be more accurate if to take into account the long-range electron correlation (London dispersion interactions).

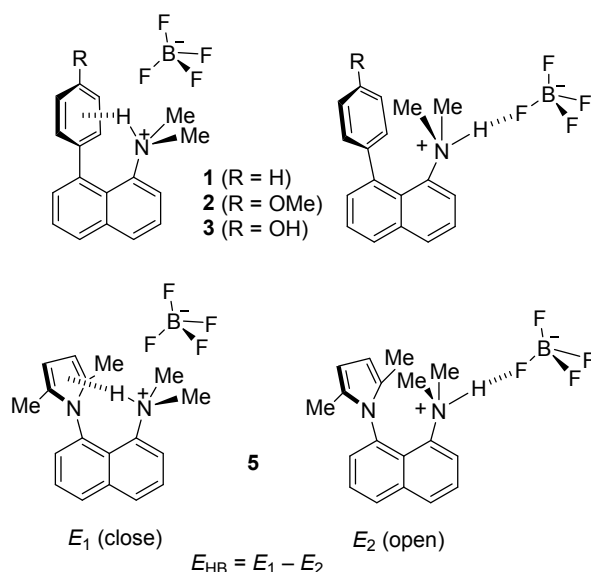
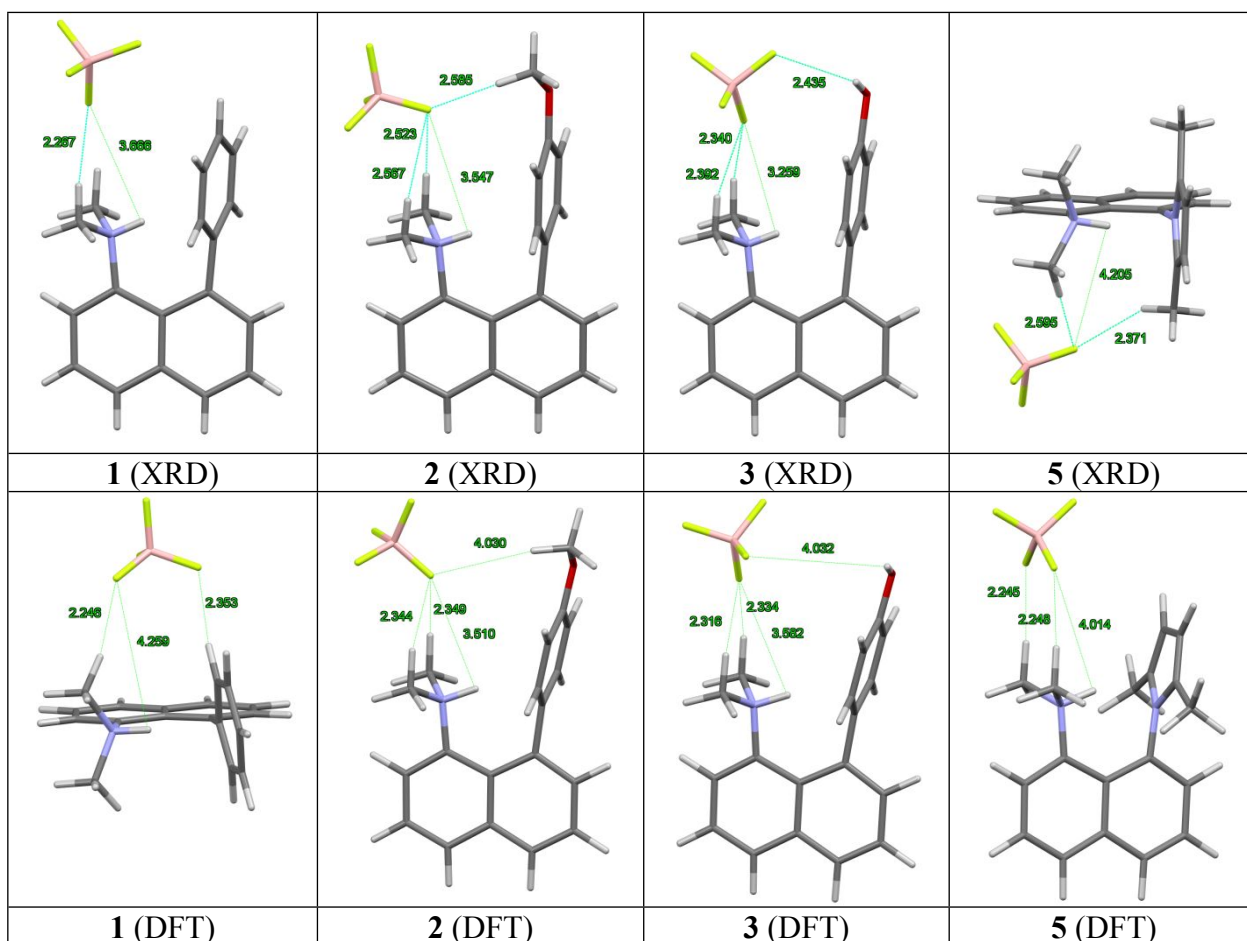


**Figure 9.** Structures with close and open IHBs used for calculation of  $E_{\text{HB}}$  values (at calculation of the “naked” cations, the  $\text{BF}_4^-$  anion was omitted).

When considering salts like **1–3** and **5**, the main drawback of the “rotational” approach is the existence of hydrogen bonds between the anion  $\text{X}^-$  ( $\text{BF}_4^-$  in our case) and acidic protons, not only in the close, but also in the open forms. Even more important is the fact that character of the hydrogen bonding in both forms is essentially different. In the close forms, the NH proton is strongly shielded by both *peri*-substituents, which keeps it at a considerable distance from the anion and thus minimizes the  $\text{NH}\dots\text{X}^-$  bifurcation interactions (see above discussion concerning solid state XRD measurements). Instead, as it was shown for proton sponge salts, the  $\text{CH}\dots\text{X}^-$  hydrogen bonds between the anion and the H-atoms play a significant role since up to 40% of the positive charge is concentrated on the *N*-methyl groups due to dispersion.<sup>27</sup> According to XRD studies and the theoretical calculations, the  $\text{CH}\dots\text{X}^-$  interactions are also important in salts **1–3**, **5** (Table 4). This is evidenced by both the location of the  $\text{BF}_4^-$  anion over the *N*-methyl groups and the distances  $\text{CH}\dots\text{F}$ , which are noticeably shorter than the sum of the van der Waals radii of the hydrogen and fluorine atoms. In fact, the situation is complicated even more owing to interactions of the  $\text{BF}_4^-$  anion with the CH bonds of the aromatic rings (compound **1**), methoxy (**2**) and C–CH<sub>3</sub> groups (**5**), as well as the OH proton (**3**).

**Table 4.** General Views and the Shortest NH...F and CH...F Distances in Tetrafluoroborates of 1-Dimethylammonio-8-arylnaphthalenes [B3LYP/6-311++G(d,p); full version of this Table with the Grimme's D3 dispersion correction is given in ESI as Table S3]



Salt	NH...F, Å		CH...F, Å		Position of BF <sub>4</sub> <sup>-</sup> against <i>peri</i> -substituents	
	XRD	Calc. in MeCN	XRD	Calc. in MeCN	XRD	Calc. in MeCN
<b>1</b>	3.67	4.26	2.27	2.25; 2.35 <sup>a</sup>	Above H <sup>+</sup> NMe <sub>2</sub>	Aside and between both subst.
<b>2</b>	3.55	3.51	2.52; 2.57; 2.59 <sup>b</sup>	2.34; 2.35; 4.03 <sup>b</sup>	Above H <sup>+</sup> NMe <sub>2</sub>	Above H <sup>+</sup> NMe <sub>2</sub>
<b>3</b>	3.26 (3.30) <sup>c</sup>	3.58	2.34; 2.39; 2.44 <sup>d</sup>	2.32; 2.33; 4.03 <sup>d</sup>	Above H <sup>+</sup> NMe <sub>2</sub>	Above H <sup>+</sup> NMe <sub>2</sub>
<b>5</b>	4.21	4.01	2.60; 2.37 <sup>e</sup>	2.25; 2.25	Aside of the both, closer to H <sup>+</sup> NMe <sub>2</sub>	Above H <sup>+</sup> NMe <sub>2</sub>

<sup>a</sup> For *ortho*-hydrogen atom of the C<sub>6</sub>H<sub>5</sub> group. <sup>b</sup> For CH<sub>3</sub>O. <sup>c</sup> Average value for two of four independent molecules (see Table 1). <sup>d</sup> For OH...F. <sup>e</sup> For C-Me.

Unlike chelated forms, in the open ones the NH proton is not sterically shielded, so its bond with the anion becomes much shorter and rather strong. As a result, the difference  $E = E_1 - E_2$  characterizes

not so much the hydrogen bond energy in the chelated cation as the difference in the energy of all noncovalent interactions in the two forms. Obviously, this circumstance should manifest itself in an underestimation of the  $E_{\text{HB}}$  values and make the latter less reliable, especially for the gas-phase state. The data in Table 5 confirm this assumption, and for salt **5**, the calculation even predicts greater stability of the open form. In addition, the sequence of salts with respect to the  $E_{\text{HB}}$  values is not consistent with XRD data and looks very irrational. Indeed, at the end of the row given below is salt **5**, although the 2,5-dimethyl-1-pyrrolyl group is a stronger  $\pi$ -donor than *p*-hydroxyphenyl, *p*-anisyl, and especially phenyl.

*Calculated gas-phase hydrogen bond energies,  $E_{\text{HB}}$*

Without Grimme's correction: **1** > **3** > **2** > **5**

With Grimme's correction: **3** > **2** > **1** > **5**

**Table 5.** Calculated NH... $\pi$  Bond Energies in Tetrafluoroborates **1–3** and **5** [B3LYP/6-311++G(d,p) and B3LYP-D3/6-311++G(d,p)]

Salt	Medium	$E_{\text{HB}}$ , kcal mol <sup>-1</sup>		NH...FBF <sub>3</sub> <sup>-</sup> distance, Å			
		B3LYP/6-311++G(d,p)	B3LYP-D3/6-311++G(d,p)	B3LYP/6-311++G(d,p)		B3LYP-D3/6-311++G(d,p)	
				Close	Open	Close	Open
<b>1</b>	Gas phase	-6.53 -6.24 ZPE <sup>a</sup>	-4.49 -4.30 ZPE	1.906	1.667	2.079	1.731
<b>1</b>	MeCN	-8.56 -8.53 ZPE	-5.71 -5.95 ZPE	4.259	1.782	4.576	1.754
<b>2</b>	Gas phase	-2.57 -2.48 ZPE	-4.96 -4.69 ZPE	1.927	1.619	2.107	1.619
<b>2</b>	MeCN	-7.34 -7.32 ZPE	-6.79 -6.81 ZPE	3.510	1.775	2.987	1.774
<b>3</b>	Gas phase	-2.74 -2.62 ZPE	-5.13 -4.85 ZPE	1.925	1.617	2.100	1.616
<b>3</b>	MeCN	-7.29 -7.41 ZPE	-9.76 -9.55 ZPE	3.582	1.771	3.384	1.753
<b>5</b>	Gas phase	0.93 0.43 ZPE	0.39 -0.16 ZPE	2.078	1.637	2.010	1.698
<b>5</b>	MeCN	-7.47 -7.84 ZPE	-6.24 -6.39 ZPE	4.014	1.780	3.481	1.749

<sup>a</sup> Energy values corrected for zero-point energy and taken as  $(E_0 + E_{\text{zpe}})_{\text{close}} - (E_0 + E_{\text{zpe}})_{\text{open}}$ .

In terms of the absolute values of  $E_{\text{HB}}$ , the calculation for acetonitrile solutions turned out to be more reliable, what can be assigned to the ionic associates and hydrogen bonds loosening, especially in the open forms. Such calculations rank the studied compounds with regard to the NH... $\pi$  hydrogen bond strength in the following order (ZPE):

1  
2  
3  
4  
5  
6  
7  
8  
9  
10  
11  
12  
13  
14  
15  
16  
17  
18  
19  
20  
21  
22  
23  
24  
25  
26  
27  
28  
29  
30  
31  
32  
33  
34  
35  
36  
37  
38  
39  
40  
41  
42  
43  
44  
45  
46  
47  
48  
49  
50  
51  
52  
53  
54  
55  
56  
57  
58  
59  
60

Calculated hydrogen bond energies,  $E_{HB}$ , in MeCN medium

Without Grimme's correction: **1 > 5 > 3 > 2**

With Grimme's correction: **3 > 2 > 5 > 1**

The first place of salt **1** in the upper sequence is doubtful since a phenyl group is the weakest  $\pi$ -donor among all. Calculations with the Grimme's correction provide more reliable sequence (lower line) though the third position of salt **5** is still questionable. To exemplify the manifestation of the Grimme's dispersion correction let us consider tetrafluoroborate salt **3**. Its optimized structure in MeCN obtained with the B3LYP/6-311++G(d,p) method demonstrates only two short CH...F contacts (Table 4 and Figure 10). In contrast, the B3LYP-D3/6-311++G(d,p) approach allows the proton donor substituent  $\text{HN}^+\text{Me}_2$  to "see" the oxygen atoms of the OH and OMe groups at a longer distances, having entered into the dispersion interaction that stabilizes the closed form. In addition, the *p*-hydroxyphenyl group in **3**, already as a proton donor, can stabilize this form via a long-distant OH...F contact with the  $\text{BF}_4^-$  anion (Figure 10). The combination of all these interactions well explains why salts **3** and **2** come to the top when using the Grimme's correction for acetonitrile solutions.

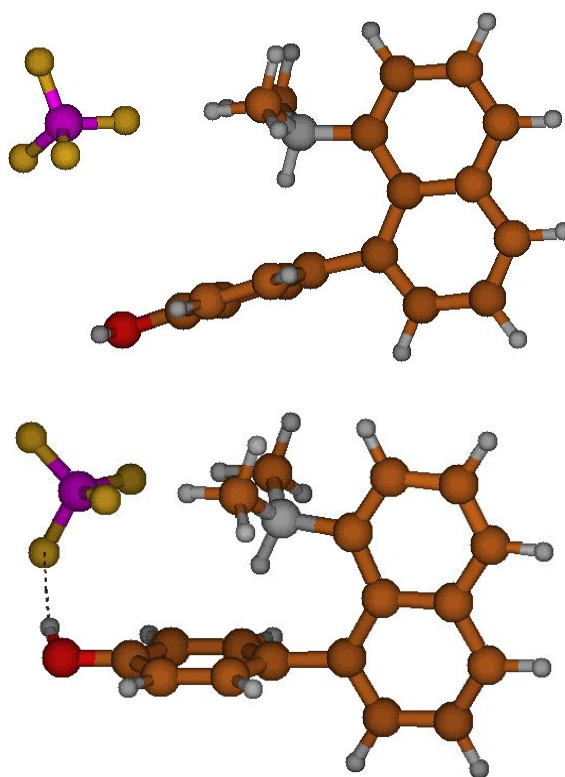


**Figure 10.** Optimized structures of salt **3** (in MeCN) obtained by B3LYP/6-311++G(d,p) (above) and B3LYP-D3/6-311++G(d,p) (below) methods.

To rule out the severe complications caused by anion-cation interactions on the NH... $\pi$  hydrogen bonds, the theoretical calculations of the “naked” cations of salts **1–3** and **5** were performed. From the results obtained (Table 6) it follows that their ranking in terms of the  $E_{\text{HB}}$  values (ZPE) in the gas phase and acetonitrile solution is exactly the same and, what is even more important, closely consistent with the relative electron donating ability of the aryl and pyrrolyl nuclei: gas phase, **5** > **2** > **3** > **1**; MeCN solution, **5** > **2** > **3** > **1**.

**Table 6.** Comparison of NH... $\pi$  bond energies in "naked" cations calculated by B3LYP/6-311++G(d,p) and B3LYP-D3/6-311++G(d,p)\*

Cation	Medium	$E_{\text{HB}}$ , kcal mol <sup>-1</sup>	$E_{\text{HB}}$ , kcal mol <sup>-1*</sup>
<b>1</b>	Gas phase	-13.69 -13.77 ZPE	-13.19 -13.48 ZPE
<b>1</b>	MeCN	-11.73 -11.83 ZPE	-11.10 -11.24 ZPE
<b>2</b>	Gas phase	-14.10 -14.28 ZPE	-13.62 -13.90 ZPE
<b>2</b>	MeCN	-12.03 -12.28 ZPE	-11.41 -11.52 ZPE
<b>3</b>	Gas phase	-13.93 -14.10 ZPE	-13.43 -13.70 ZPE
<b>3</b>	MeCN	-11.95 -12.19 ZPE	-11.31 -11.55 ZPE
<b>5</b>	Gas phase	-14.98 -15.34 ZPE	-15.28 -15.55 ZPE
<b>5</b>	MeCN	-12.07 -12.29 ZPE	-11.95 -12.28 ZPE

As expected, the  $E_{\text{HB}}$  values in the “naked” cations in acetonitrile are significantly larger than in tetrafluoroborate salts. This fact seems to be important as it underlines how large can be the influence of the environment on the NH... $\pi$  binding in living tissues. One can think that when the NH... $\pi$  binding is realized in a hydrophobic environment, charged proton donors such as ammonium groups behave similar to “naked” cations. In such a case, according to our calculations, the energy of the NH... $\pi$  interactions can reach 12–15 kcal mol<sup>-1</sup>, while in the polar environment (water and various anions) it decreases by at least 4–5 kcal mol<sup>-1</sup>. As can be seen from Table 6 (right column), in the case of “naked” cations, the inclusion of the dispersion factor does not bring any changes to their arrangement in terms of  $E_{\text{HB}}$  values (**5** > **2** > **3** > **1**). The only difference is a slight decrease in the hydrogen bond strength (by 0.2–0.7 kcal mol<sup>-1</sup>) for cations **1–3** (a slight increase was obtained only for cation **5** in the gas phase).

## Conclusions

On the whole, in order to simulate NH... $\pi$  interactions involved in the stabilization of the secondary and tertiary structure of proteins, the molecular structures of nine representatives of *peri*-disubstituted naphthalenes were examined in the solid state and MeCN solution. According to both the XRD and  $^1\text{H}$  NMR measurements, the  $\pi$ -donor activity of the studied substituents decreases in the following sequence: 2,5-dimethyl-1-pyrrolyl > 4-hydroxyphenyl > phenyl > *p*-anisyl > 2-naphthyl, while the largest proton donor ability is characterized by the  $\text{Me}_2\text{NH}^+$  group, which significantly exceeds those of the neutral  $\text{NH}_2$  group and pyridinium  $\text{N-H}^+$  bond. No NH... $\pi$  interaction has been observed in 1-acetamido-8-phenylnaphthalene. DFT calculations of the energy of the NH... $\pi$  hydrogen bond,  $E_{\text{HB}}$ , in tetrafluoroborates **1–3** and **5** revealed a strong distorting effect caused by the counterion. At the same time, the  $E_{\text{HB}}$  values for "naked" cations, lying between 13.5–15.5 (in the gas phase) and 11.2–12.3 kcal mol $^{-1}$  (for MeCN solution) look quite reasonable, agreeing with the XRD and NMR sequences. The dominant position of the 2,5-dimethyl-1-pyrrolyl group reflects the ideal pre-organization of the latter for NH... $\pi$  interaction, the highest linearity of the NH... $\pi$  bond and the record short NH...N and NH...centroid distances (2.07 Å).

## Experimental Section

**General.** Solution  $^1\text{H}$  and  $^{13}\text{C}$  NMR experiments were performed with a 600 MHz, 300 MHz or 250 MHz spectrometers. Mass spectra were obtained from Finnigan MAT INCOS 50 instrument (electron impact, 70 eV). The HR-ESI mass-spectra were obtained on a BRUKER maXis spectrometer equipped with an electrospray ionization (ESI) source; methanol was used as the solvent (Chemical Analysis and Materials Research Centre, St. Petersburg State University). The instrument was operated in positive mode using an  $m/z$  range of 50–1200. The capillary voltage of the ion source was set at 4000 V. The nebulizer gas pressure was 1.0 bar, and the drying gas flow was set to 4.0 L/min. IR spectra were recorded on an FT FSM-1202 spectrometer. All reagents and starting materials were obtained from commercial sources and used without further purification. Tetrafluoroborate **1** and *N,N*-dimethyl-8-phenylnaphthalen-1-amine (**13**) were synthesized as described previously.<sup>7</sup>

***N*-(8-(4-Methoxyphenyl)naphthalene-1-yl)acetamide (10):** A solution of  $\text{Na}_2\text{CO}_3 \cdot 10\text{H}_2\text{O}$  (2.05 g, 7 mmol) in water (10 mL) was added under argon to a solution of *N*-(8-bromonaphthalen-1-yl)acetamide (**9**)<sup>9</sup> (1.27 g, 4.8 mmol), 4-methoxyphenylboronic acid (0.9 g, 6 mmol), palladium acetate (23 mg, 0.1 mmol) and triphenylphosphane (75 mg, 0.3 mmol) in propanol (25 mL). The resulting mixture was heated on a silicone oil bath at reflux for 6 h. The solvent was evaporated in vacuum and water was

1 added to the residue. The mixture was extracted with  $\text{CHCl}_3$  and the crude product obtained after  
2 solvent evaporation was purified by column chromatography ( $\text{Al}_2\text{O}_3/\text{CHCl}_3$ ) ( $R_f$  0.6) to give **10** (0.76 g;  
3 54%) as beige crystals; m.p. 141–142 °C.  $^1\text{H}$  NMR (250 MHz,  $\text{CDCl}_3$ ):  $\delta$  = 1.51 (s, 3H, Ac), 3.87 (s,  
4 3H, OMe), 7.02 (d,  $J$  = 8.6 Hz, 2H), 7.19 (s, 1H, NH), 7.25 (s,  $J$  = 6.2 Hz, 1H), 7.34 (d,  $J$  = 8.5 Hz,  
5 2H), 7.40–7.50 (m, 2H), 7.71 (d,  $J$  = 8.1 Hz, 1H), 7.84 (d,  $J$  = 8.1 Hz, 1H), 8.07 (d,  $J$  = 7.5 Hz, 1H).  
6  $^{13}\text{C}\{^1\text{H}\}$  NMR (62.9 MHz,  $\text{CDCl}_3$ ):  $\delta$  = 24.3, 55.6, 114.1, 121.3, 124.1, 124.7, 125.8, 125.9, 128.9,  
7 130.1, 130.2, 133.2, 135.3, 135.5, 136.4, 159.3, 167.8 ppm. IR (nujol,  $\text{cm}^{-1}$ ): 3246 (NH), 1700 (C=O).  
8 MS:  $m/z$  (%) = 291 (100)  $[\text{M}]^+$ , 249 (99), 234 (35), 217 (26), 204 (78). Anal. calcd: C 78.33, H 5.88, N  
9 4.81;  $\text{C}_{19}\text{H}_{17}\text{NO}_2$ ; found: C 78.53, H 5.69, N 4.60.

10  
11  
12  
13  
14  
15  
16  
17  
18 **8-(4-Methoxyphenyl)naphthalene-1-amine (7)**: A mixture of compound **10** (690 mg, 2.4 mmol),  
19 ethanol (2.5 mL) and conc. hydrochloric acid (1.2 mL) was heated on a silicone oil bath at reflux for 3  
20 h. After evaporation of the solvents, the residue was stirred with  $\text{Et}_2\text{O}$  (3 mL) and a solution of KOH  
21 (300 mg) in water (2 mL) until the solid was completely dissolved. The organic layer was separated  
22 and the aqueous layer was extracted with  $\text{Et}_2\text{O}$  (3 x 2 mL). The combined organic layers were  
23 evaporated to afford **7** (568 mg, 96%) as beige crystals; m.p. 98–99 °C.  $^1\text{H}$  NMR (250 MHz,  $\text{CDCl}_3$ ):  $\delta$   
24 = 3.52 (s, 2H,  $\text{NH}_2$ ), 3.87 (s, 3H, OMe), 6.63 (dd,  $J$  = 7.1, 1.5 Hz, 1H), 6.96–6.99 (m, 2H), 7.15 (dd,  $J$  =  
25 7.0, 1.2 Hz, 1H), 7.27–7.41 (m, 5H), 7.77 (dd,  $J$  = 8.2, 1.1 Hz, 1H).  $^{13}\text{C}\{^1\text{H}\}$  NMR (62.9 MHz,  $\text{CDCl}_3$ ):  
26  $\delta$  = 55.4, 111.2, 113.5, 119.0, 121.0, 124.7, 126.6, 128.5, 128.6, 130.4, 135.7, 136.0, 138.0, 143.9,  
27 159.1 ppm. IR (nujol,  $\text{cm}^{-1}$ ): 3456, 3357 ( $\text{NH}_2$ ). MS:  $m/z$  (%) = 249 (100)  $[\text{M}]^+$ , 234 (30), 217 (16), 204  
28 (43). Anal. calcd: C 81.90, H 6.06, N 5.62;  $\text{C}_{17}\text{H}_{15}\text{NO}$ ; found: C 82.13, H 6.29, N 5.33.

29  
30  
31  
32  
33  
34  
35  
36  
37 ***N*-(1,2'-Binaphthyl-8-yl)acetamide (11)**: A solution of  $\text{Na}_2\text{CO}_3 \cdot 10\text{H}_2\text{O}$  (130 mg, 0.45 mmol) in water  
38 (1 mL) was added under argon to a solution of *N*-(8-bromonaphthalen-1-yl)acetamide (**9**) (100 mg,  
39 0.38 mmol), 2-naphthylboronic acid (65 mg, 0.38 mmol), palladium acetate (1 mg, 0.004 mmol) and  
40 triphenylphosphane (4 mg, 0.015 mmol) in propanol (3 mL). The resulting mixture was heated on a  
41 silicone oil bath at reflux for 6 h. The solvent was evaporated in vacuum and water was added to the  
42 residue. The mixture was extracted with  $\text{CHCl}_3$  and the crude product obtained after solvent  
43 evaporation was purified by column chromatography ( $\text{Al}_2\text{O}_3/\text{CHCl}_3$ ) to obtain **11** ( $R_f$  0.6) (77 mg;  
44 65%) as a yellow oil.  $^1\text{H}$  NMR (250 MHz,  $\text{CDCl}_3$ ):  $\delta$  = 1.03 (s, 3H, Ac), 6.97 (s, 1H, NH), 7.36 (dd,  $J$  =  
45 6.9, 0.9 Hz, 1H), 7.47–7.57 (m, 5H), 7.76 (d,  $J$  = 8.0 Hz, 1H), 7.84–7.99 (m, 6H).  $^{13}\text{C}\{^1\text{H}\}$  NMR  
46 ( $\text{CDCl}_3$ , 62.9 MHz):  $\delta$  = 23.7, 122.5, 124.6, 124.8, 126.1, 126.3, 126.7, 127.2, 127.5, 127.8, 128.0,  
47 128.1, 129.2, 130.1, 132.5, 133.0, 133.2, 135.4, 136.9, 141.0, 167.9. HRMS  $m/z$ : calc. for  $\text{C}_{22}\text{H}_{17}\text{NO} + \text{H}$   
48 312.1383, found 312.1380.  
49  
50  
51  
52  
53  
54  
55  
56  
57  
58  
59  
60

**1,2'-Binaphthyl-8-amine (14):** A mixture of compound **11** (77 mg, 0.25 mmol), ethanol (2.5 mL) and conc. hydrochloric acid (0.15 mL) was heated on a silicone oil bath at reflux for 4 h. After evaporation of the solvents, the residue was stirred with CH<sub>2</sub>Cl<sub>2</sub> (1 mL) and 0.1 M KOH (1 mL) until the solid was completely dissolved. The organic layer was separated and the aqueous layer extracted with CH<sub>2</sub>Cl<sub>2</sub> (3 x 2 mL). The combined organic layers were evaporated to afford **14** (54 mg, 80%) as a dark green oil. <sup>1</sup>H NMR (250 MHz, CDCl<sub>3</sub>): δ = 3.70 (s, 2H, NH<sub>2</sub>), 6.62 (dd, *J* = 7.1, 1.5 Hz, 1H), 7.21–7.24 (m, 1H), 7.26–7.44 (m, 3H), 7.52–7.60 (m, 3H), 7.81 (dd, *J* = 8.2, 1.1 Hz, 1H), 7.85–7.93 (m, 4H). <sup>13</sup>C{<sup>1</sup>H} NMR (CDCl<sub>3</sub>, 62.9 MHz): δ = 111.2, 119.0, 120.8, 124.6, 126.3, 126.6, 126.7, 127.5, 127.8, 128.0, 128.2, 128.6, 128.8, 132.5, 132.9, 136.0, 138.3, 141.2, 143.9. HRMS *m/z*: calc. for C<sub>20</sub>H<sub>15</sub>N+H 270.1277, found 270.1274.

**8-(4-Methoxyphenyl)-*N,N*-dimethylnaphthalen-1-amine (16):** A mixture of compound **7** (100 mg, 0.4 mmol), dimethyl sulfate (1.3 mL, 14 mmol), Na<sub>2</sub>CO<sub>3</sub>·10H<sub>2</sub>O (1.14 g, 4 mmol) and water (0.5 mL) was stirred at the ambient temperature for 20 h. Then the mixture was diluted with water (3 mL), extracted with CH<sub>2</sub>Cl<sub>2</sub> (3 x 2 mL), concentrated and purified by column chromatography (Al<sub>2</sub>O<sub>3</sub>/CH<sub>2</sub>Cl<sub>2</sub>) to afford **16** (*R<sub>f</sub>* 0.9) (73 mg; 66%) as a light-brown oil. <sup>1</sup>H NMR (CDCl<sub>3</sub>, 250 MHz): δ = 2.26 (s, 6H, NMe<sub>2</sub>), 3.86 (s, 3H, OMe), 6.81–6.87 (m, 2H), 7.03 (d, *J* = 7.2 Hz, 1H), 7.29–7.47 (m, 5H), 7.54 (dd, *J* = 8.1, 1.1 Hz, 1H), 7.77 (dd, *J* = 8.1, 1.3 Hz, 1H). <sup>13</sup>C{<sup>1</sup>H} NMR (CDCl<sub>3</sub>, 62.9 MHz): δ = 43.4, 55.3, 111.4, 115.1, 123.0, 125.0, 125.6, 125.7, 127.9, 129.6, 130.3, 136.5, 136.6, 139.3, 150.9, 157.9 ppm. MS: *m/z* (%) = 277 (62) [M]<sup>+</sup>, 262 (8), 245 (14), 234 (8), 218 (9), 203 (8), 189 (12), 57 (100), 43 (99). Anal. calcd: C 82.28, H 6.90, N 5.05; C<sub>19</sub>H<sub>19</sub>NO; found: C 82.47, H 7.19, N 5.31.

**4-(8-(Dimethylamino)naphthalen-1-yl)phenol (17):** A solution of compound **16** (100 mg, 0.36 mmol) in conc. aqueous HBr (5 mL) was heated on a silicone oil bath at reflux for 1 h, then neutralized with ammonia and extracted with CH<sub>2</sub>Cl<sub>2</sub> (3 x 5 mL). The resulting product was purified by column chromatography (Al<sub>2</sub>O<sub>3</sub>/CH<sub>2</sub>Cl<sub>2</sub>) to collect **17** (*R<sub>f</sub>* 0.4) (40 mg, 42%) as a grey oil. <sup>1</sup>H NMR (250 MHz, CDCl<sub>3</sub>): δ = 2.26 (s, 6H, NMe<sub>2</sub>), 5.29 (d, *J* = 1.5 Hz, 1H), 6.79 (d, *J* = 8.5 Hz, 2H), 7.03 (d, *J* = 6.7 Hz, 1H), 7.23–7.31 (m, 3H), 7.36–7.45 (m, 2H), 7.54 (d, *J* = 7.4 Hz, 1H), 7.77 (dd, *J* = 8.0, 1.0 Hz, 1H). <sup>13</sup>C{<sup>1</sup>H} NMR (CDCl<sub>3</sub>, 62.9 MHz): δ = 43.4, 113.0, 115.1, 122.9, 125.0, 125.6, 125.7, 128.0, 129.5, 130.5, 136.6, 136.7, 139.3, 150.9, 153.9. HRMS *m/z*: calc. for C<sub>18</sub>H<sub>17</sub>NO 264.1383, found 264.1384. IR (CCl<sub>4</sub>, cm<sup>-1</sup>): 3611 (OH).

***N,N*-Dimethyl-1,2'-binaphthyl-8-amine (18):** A mixture of compound **14** (53 mg, 0.2 mmol), dimethyl sulfate (0.66 mL, 7 mmol), Na<sub>2</sub>CO<sub>3</sub>·10H<sub>2</sub>O (572 mg, 2 mmol) and water (1 mL) was stirred at room temperature for 24 h. The crude mixture was neutralized with ammonia and extracted with CH<sub>2</sub>Cl<sub>2</sub> (3 x 2 mL). Purification by column chromatography (Al<sub>2</sub>O<sub>3</sub>/CH<sub>2</sub>Cl<sub>2</sub>) afforded amine **18** (*R<sub>f</sub>* 0.9)

(47 mg; 80%) as a brown oil.  $^1\text{H}$  NMR (250 MHz,  $\text{CDCl}_3$ ):  $\delta$  = 1.99 (br. s, 3H, N-Me<sup>a</sup>), 2.38 (br. s, 3H, N-Me<sup>b</sup>), 7.08 (d, 1H), 7.42–7.49 (m, 6H), 7.60 (d,  $J$  = 8.0 Hz, 1H), 7.66 (d,  $J$  = 8.5 Hz, 1H), 7.82–7.89 (m, 3H), 7.95 (s, 1H).  $^{13}\text{C}\{^1\text{H}\}$  NMR ( $\text{CDCl}_3$ , 62.9 MHz):  $\delta$  = 115.8, 123.4, 124.0, 125.2, 125.3, 125.3, 125.5, 125.9, 126.3, 127.4, 127.9, 128.4, 129.9, 130.0, 132.1, 132.9, 136.5, 139.6, 142.5, 151.1. HRMS  $m/z$ : calc. for  $\text{C}_{20}\text{H}_{15}\text{N}+\text{H}$  298.1590, found 298.1590.

***N*-Methyl-*N*-(8-phenylnaphthalen-1-yl)acetamide (19)**: Potassium hydroxide (112 mg, 2 mmol) was stirred in dimethyl sulfoxide (3 mL) until dissolution, then *N*-(8-phenylnaphthalen-1-yl)acetamide (**8**)<sup>8</sup> (464 mg, 1.8 mmol) and methyl iodide (0.4 mL, 6.4 mmol) were added and the reaction mixture was stirred at room temperature for 24 h. The resulting product was separated on addition of water (50 mL), filtered off and purified by column chromatography ( $\text{Al}_2\text{O}_3/\text{CH}_2\text{Cl}_2$ ) to give colorless crystals of **19** (170 mg, 35%). M.p. 170–170.2 °C;  $^1\text{H}$  NMR (250 MHz,  $\text{CDCl}_3$ ):  $\delta$  = 1.50 (s, 0.5H,  $\text{CH}_3$ ), 1.70 (s, 3H,  $\text{CH}_3$ ), 2.63 (s, 3H,  $\text{CH}_3$ ), 2.78 (s, 0.5H,  $\text{CH}_3$ ), 7.18–7.20 (m, 1.7H), 7.26–7.29 (m, 1.2H), 7.33–7.38 (m, 5H), 7.45–7.55 (m, 2.6H), 7.85–7.94 (m, 2.3H).  $^{13}\text{C}\{^1\text{H}\}$  NMR ( $\text{CDCl}_3$ , 62.9 MHz):  $\delta$  = 22.0, 23.1, 37.8, 40.5, 125.1, 125.6, 125.8, 125.9, 126.5, 127.0, 127.1, 127.5, 127.6, 127.8, 128.1, 128.3, 128.4, 128.9, 129.2, 129.6, 130.7, 131.3, 136.0, 138.4, 140.9, 142.6, 170.6, 171.6 ppm. MS:  $m/z$  (%) = 275 (45)  $[\text{M}]^+$ , 233 (40), 216 (56), 202 (15), 189 (11), 56 (100), 43 (74). Anal. calcd: C 82.88, H 6.22, N 5.09.  $\text{C}_{19}\text{H}_{17}\text{NO}$ ; found: C 83.09, H 6.02, N 5.30.

***N*-(8-(4-Methoxyphenyl)naphthalen-1-yl)-*N*-methylacetamide (20)**: Potassium hydroxide (100 mg, 1.8 mmol) was stirred in dimethyl sulfoxide (3 mL) until dissolution, then *N*-(8-(4-methoxyphenyl)naphthalen-1-yl)acetamide (**10**) (450 mg, 1.55 mmol) and methyl iodide (0.5 mL, 8 mmol) were added and the reaction mixture was stirred at room temperature for 24 h. The resulting product was separated on addition of water (50 mL), filtered off and purified by column chromatography ( $\text{Al}_2\text{O}_3/\text{CH}_2\text{Cl}_2$ ) to afford **20** (238 mg, 50%) as colorless crystals. M.p. 191–193.5 °C;  $^1\text{H}$  NMR (250 MHz,  $\text{CDCl}_3$ ):  $\delta$  = 1.59 (s, 0.6H,  $\text{CH}_3$ ), 1.70 (s, 3H,  $\text{CH}_3$ ), 2.64 (s, 3H,  $\text{CH}_3$ ), 2.77 (s, 0.6H,  $\text{CH}_3$ ), 3.82 (s, 3H,  $\text{OCH}_3$ ), 3.83 (s, 0.6H,  $\text{OCH}_3$ ), 6.87–6.90 (m, 2.2H), 7.12–7.19 (m, 3H), 7.22–7.25 (m, 0.4H), 7.28–7.32 (m, 1.4H), 7.40–7.52 (m 2.4H), 7.82–7.92 (m, 2.4H).  $^{13}\text{C}\{^1\text{H}\}$  NMR ( $\text{CDCl}_3$ , 62.9 MHz):  $\delta$  = 22.2, 23.0, 37.8, 40.4, 55.3, 55.4, 112.5, 112.8, 112.9, 113.2, 125.1, 125.6, 125.7, 125.8, 127.5, 128.4, 128.8, 128.8, 129.0, 129.1, 129.5, 129.6, 130.4, 131.0, 131.7, 134.9, 135.7, 136.0, 137.6, 138.2, 140.5, 141.0, 158.4, 158.6, 170.5, 171.5 ppm. MS:  $m/z$  (%) = 305 (94)  $[\text{M}]^+$ , 291 (16), 263 (40), 248 (35), 231 (17), 216 (30), 204 (57), 189 (24), 56 (89), 43 (100). Anal. calcd: C 78.66, H 6.27, N 4.59;  $\text{C}_{20}\text{H}_{19}\text{NO}_2$ ; found: C 78.29, H 6.47, N 4.29.

**8-(2,5-Dimethyl-1*H*-pyrrol-1-yl)-*N,N*-dimethylnaphthalen-1-amine (24).** A mixture of *N,N*-dimethylnaphthalene-1,8-diamine (**23**) (44 mg, 0.24 mmol) and 2,5-hexanedione (70  $\mu$ L, 0.6 mmol) was heated on a silicone oil bath at 145–150  $^{\circ}$ C for 3 h. Then the reaction mixture was cooled down to the ambient temperature, diluted with  $\text{CH}_2\text{Cl}_2$  (2 mL) and subjected to column chromatography ( $\text{Al}_2\text{O}_3/\text{CHCl}_3$ –hexane, 1:3) to afford compound **24** ( $R_f$  0.4) (20 mg; 32%) as light brown crystals with m.p. 41–43  $^{\circ}$ C.  $^1\text{H}$  NMR ( $\text{CD}_3\text{CN}$ , 600 MHz):  $\delta$  = 1.89 (s, 6H), 2.40 (s, 6H), 5.79 (s, 2H), 7.15 (dd,  $J$  = 7.24, 1.33 Hz, 1H), 7.20 (dd,  $J$  = 7.47, 1.15 Hz, 1H), 7.43–7.45 (m, 1H), 7.51 (dd,  $J$  = 8.17, 7.25 Hz, 1H), 8.64–8.65 (m, 1H), 7.91–7.92 (m, 1H).  $^{13}\text{C}\{^1\text{H}\}$  NMR ( $\text{CD}_3\text{CN}$ , 150 MHz):  $\delta$  = 12.78, 44.89, 105.39, 117.31, 124.14, 125.49, 126.29, 126.61, 129.03, 129.42, 129.78, 135.09, 137.47, 151.52 ppm. HRMS  $m/z$ : calc. for  $\text{C}_{18}\text{H}_{20}\text{N}_2+\text{H}$  256.1699, found 265.1704.

**General Procedure for Preparation of Proton Complexes With Tetrafluoroboric Acid (Hydrogen Tetrafluoroborates) (2–6, 31).** These were prepared by mixing equimolar amounts of appropriate bases and 40% aqueous  $\text{HBF}_4$  in a minimum volume of EtOAc followed by 3-fold dilution with  $\text{Et}_2\text{O}$ . The residue thus formed was washed with  $\text{Et}_2\text{O}$  and vacuum-dried to give the desired salts in high yield.

**8-(4-Methoxyphenyl)-*N,N*-dimethylnaphthalen-1-aminium Tetrafluoroborate (2).** Obtained from compound **16** (92 mg, 0.33 mmol) according to general procedure. Colorless crystals of **2** (89 mg, 73%) with m.p. 127–129  $^{\circ}$ C.  $^1\text{H}$  NMR ( $\text{CD}_3\text{CN}$ , 300 MHz):  $\delta$  = 3.08 (d,  $J$  = 5.3 Hz, 6H,  $\text{NMe}_2$ ), 3.97 (s, 3H, OMe), 7.28 (d,  $J$  = 8.7 Hz, 2H), 7.52 (dd,  $J$  = 7.1, 1.1 Hz, 1H), 7.61 (d,  $J$  = 8.7 Hz, 2H), 7.71–7.80 (m, 2H), 7.93 (d,  $J$  = 7.3 Hz, 1H), 8.16 (dd,  $J$  = 8.3, 0.8 Hz, 1H), 8.25 (d,  $J$  = 8.1 Hz, 1H), 8.45 (s, 1H, NH).  $^{13}\text{C}\{^1\text{H}\}$  NMR ( $\text{CD}_3\text{CN}$ , 75.5 MHz):  $\delta$  = 47.9, 55.9, 116.7, 121.0, 123.2, 126.5, 127.3, 130.2, 130.8, 131.0, 132.7, 133.0, 134.4, 135.9, 139.7, 162.1. Anal. calcd: C 62.49, H 5.52, N 3.84;  $\text{C}_{19}\text{H}_{20}\text{BF}_4\text{NO}$ ; found: C 62.72, H 5.28, N 3.52.

**8-(4-Hydroxyphenyl)-*N,N*-dimethylnaphthalen-1-aminium Tetrafluoroborate (3):** Obtained from compound **17** (26 mg, 0.1 mmol) according to general procedure. Colorless crystals of **3** (29 mg, 83%) with m.p. 169–170  $^{\circ}$ C.  $^1\text{H}$  NMR ( $\text{CD}_3\text{CN}$ , 300 MHz):  $\delta$  = 3.08 (d,  $J$  = 5.3 Hz, 6H,  $\text{NMe}_2$ ), 7.15–7.18 (m, 2H), 7.50–7.54 (m, 3H), 7.70–7.79 (m, 3H), 7.91 (dd,  $J$  = 7.7, 0.8 Hz, 1H), 8.15 (dd,  $J$  = 8.3, 1.1 Hz, 1H), 8.24 (d,  $J$  = 8.2 Hz, 1H), 8.57 (br. s, 1H, NH).  $^{13}\text{C}\{^1\text{H}\}$  NMR ( $\text{CD}_3\text{CN}$ , 75.5 MHz):  $\delta$  = 47.8, 120.9, 123.1, 126.5, 127.3, 129.9, 130.1, 131.1, 132.7, 133.0, 134.5, 135.8, 139.6, 159.7. Anal. calcd: C 61.57, H 5.17, N 3.99;  $\text{C}_{18}\text{H}_{18}\text{BF}_4\text{NO}$ ; found: C 61.80, H 5.32, N 3.70.

***N,N*-Dimethyl-1,2'-binaphthyl-8-aminium Tetrafluoroborate (4):** Obtained from compound **18** (30 mg, 0.1 mmol) according to general procedure. Light-brown crystals of **4** (34 mg, 88%) with m.p. 194–

195 °C. <sup>1</sup>H NMR (CD<sub>3</sub>CN, 250 MHz): δ = 3.00 (d, *J* = 5.2 Hz, 3H, N-Me<sup>a</sup>), 3.07 (d, *J* = 5.2 Hz, 3H, N-Me<sup>b</sup>), 7.66 (dd, *J* = 7.1, 1.1 Hz, 1H), 7.73–7.86 (m, 5H), 7.98 (d, *J* = 7.6 Hz, 1H), 8.08–8.11 (m, 1H), 8.15–8.19 (m, 1H), 8.23–8.34 (m, 4H). <sup>13</sup>C{<sup>1</sup>H} NMR (CD<sub>3</sub>CN, 62.9 MHz): δ = 47.4, 47.4, 120.6, 122.3, 125.7, 126.1, 126.8, 128.0, 128.1, 128.3, 128.3, 128.6, 129.9, 131.1, 132.3, 132.8, 133.6, 134.0, 134.1, 135.4, 136.3, 139.0 ppm. Anal. calcd: C 68.60, H 5.23, N 3.64; C<sub>22</sub>H<sub>20</sub>BF<sub>4</sub>N; found: C 68.41, H 5.55, N 3.36.

**8-(2,5-Dimethyl-1H-pyrrol-1-yl)-N,N-dimethylnaphthalen-1-aminium Tetrafluoroborate (5):**

Obtained from compound **25** (23 mg, 0.09 mmol) according to general procedure. Brown crystals of **5** (27 mg, 87%) with m.p. 168–171 °C. <sup>1</sup>H NMR (CD<sub>3</sub>CN, 600 MHz): δ = 1.96 (s, 6H, 2C-Me), 3.16 (d, *J* = 5.09 Hz, 6H, NMe<sub>2</sub>), 6.21 (br. s, 1H, NH), 6.30 (s, 2H), 7.71 (dd, *J* = 7.26, 1.30 Hz, 1H), 7.78–7.84 (m, 2H), 8.01 (dd, *J* = 7.82, 1.01 Hz, 1H), 8.27 (ddd, *J* = 8.35, 1.29, 0.43 Hz, 1H), 7.29 (dd, *J* = 8.22, 1.04 Hz, 1H). <sup>13</sup>C{<sup>1</sup>H} NMR (CD<sub>3</sub>CN, 150 MHz): δ = 11.87, 50.45, 110.28, 122.29, 122.39, 127.07, 127.67, 129.93, 130.32, 131.69, 131.83, 132.84, 136.53, 138.25 ppm. Anal. calcd: C 61.39, H 6.01, N 7.95; C<sub>18</sub>H<sub>21</sub>BF<sub>4</sub>N<sub>2</sub>; found: C 61.11, H 6.25, N 8.09.

**10-Phenylbenzo[*h*]quinolinium Tetrafluoroborate (6):** Obtained from compound **22** (33 mg, 0.13

mmol) according to general procedure. Yellowish crystals of **6** (36 mg, 82%) with m.p. 216–218 °C. <sup>1</sup>H NMR (CD<sub>3</sub>CN, 300 MHz): δ = 7.64–7.66 (m, 2H), 7.72–7.75 (m, 3H), 7.77 (dd, *J* = 7.4, 1.3 Hz, 1H), 8.02–8.12 (m, 2H), 8.17 (d, *J* = 8.9 Hz, 1H), 8.27 (dd, *J* = 8.1, 1.2 Hz, 1H), 8.35 (d, *J* = 8.9 Hz, 1H), 8.60 (dd, *J* = 5.7, 1.6 Hz, 1H), 9.18 (dd, *J* = 8.2, 1.6 Hz, 1H), 12.35 (br. s, 1H, NH). <sup>13</sup>C{<sup>1</sup>H} NMR (CD<sub>3</sub>CN, 75.5 MHz): δ = 119.7, 123.0, 125.1, 129.7, 129.8, 130.1, 130.3, 130.6, 131.4, 132.3, 133.6, 136.5, 137.4, 138.7, 139.2, 141.2, 147.6. Anal. calcd: C 66.51, H 4.11, N 4.08; C<sub>19</sub>H<sub>14</sub>BF<sub>4</sub>N; found: C 66.43, H 4.09, N 3.98.

**10,10'-Dibenzo[*h*]quinolinium Bis(tetrafluoroborate) (31):** Obtained from 10,10'-

dibenzo[*h*]quinoline<sup>14</sup> (44 mg, 0.12 mmol) according to general procedure. Yellowish crystals of **31** (52 mg, 81%) not melting up to 290 °C. <sup>1</sup>H NMR (CD<sub>3</sub>CN, 300 MHz): δ = 7.75 (dd, *J* = 7.5, 1.3 Hz, 2H), 8.05 (t, *J* = 7.5 Hz, 2H), 8.11 (dd, *J* = 8.4, 5.7 Hz, 2H), 8.33 (d, *J* = 8.9 Hz, 2H), 8.51–8.54 (m, 4H), 8.57 (dd, *J* = 5.7, 1.5 Hz, 2H), 9.25 (dd, *J* = 8.4, 1.5 Hz, 2H), 12.50 (very br. s, 2H, NH). Anal. calcd: C 58.70, H 3.41, N 5.27; C<sub>26</sub>H<sub>18</sub>B<sub>2</sub>F<sub>8</sub>N<sub>2</sub>; found: C 58.64, H 3.52, N 5.39.

**Crystal Structure Determination.** XRD measurements were conducted with Bruker APEX-II CCD diffractometer and four-circle diffractometer SuperNova, Single source at offset/far, HyPix3000. The structures were solved by direct methods and refined by the full-matrix least-squares against *F*<sup>2</sup> in anisotropic (for non-hydrogen atoms) approximation. All hydrogen atoms were placed in geometrically

1  
2 calculated positions and were refined in isotropic approximation in the riding model with the  $U_{\text{iso}}(\text{H})$   
3 parameters equal to  $n \cdot U_{\text{eq}}(\text{C}_i)$  ( $n = 1.2$  for CH and CH<sub>2</sub> groups and  $n = 1.5$  for CH<sub>3</sub> groups), where  
4  $U(\text{C}_i)$  are respectively the equivalent thermal parameters of the atoms to which corresponding H atoms  
5 are bonded. The H(N) and H(O) hydrogen atoms were found in the difference Fourier synthesis and  
6 refined in isotropic approximation. Atomic coordinates, bond lengths, bond angles and thermal  
7 parameters have been deposited at the Cambridge Crystallographic Data Centre (CCDC).

8  
9  
10  
11  
12 CCDC 1978186 (for **2**, from MeCN), 1978191 (for **3**, from MeCN), 1978190 (for **4**, from  
13 CH<sub>2</sub>Cl<sub>2</sub>/Et<sub>2</sub>O), 1978193 (for **5**, from MeCN/Et<sub>2</sub>O), 1978192 (for **6**, from MeCN), 1978189 (for **7**, from  
14 MeOH), 1978187 (for **8**, from MeCN) and 1978188 (for **31**, from CH<sub>2</sub>Cl<sub>2</sub>/acetone) contain the  
15 supplementary crystallographic data for this paper. These data can be obtained free of charge from the  
16 Cambridge Crystallographic Data Centre via [www.ccdc.cam.ac.uk/data\\_request/cif](http://www.ccdc.cam.ac.uk/data_request/cif).

17  
18  
19  
20  
21 **Theoretical Calculations.** Quantum-mechanical calculations using the B3LYP functional (DFT, the  
22 three-parameter exchange hybrid functional of Becke,<sup>28</sup> and gradient-corrected correlation functional of  
23 Lee, Yang, and Parr<sup>29</sup>) with the 6-311++G(d,p) basis set<sup>30</sup> were performed for the full geometry  
24 optimizations with the GAUSSIAN 16 program.<sup>31</sup> The associated force constants were calculated at the  
25 same level to evaluate harmonic frequencies and their zero-point energy (ZPE) corrections. The atom  
26 pair-wise correction method (DFT-D3) was also used.<sup>32</sup> Solvent effects were taken into account with  
27 the polarizable continuum model (PCM).<sup>33–35</sup>

## 28 29 30 31 32 33 34 35 **Supporting Information**

36 XRD data, spectral data, additional comments and computational details (PDF). The Supporting  
37 Information (ESI) is available free of charge on the ACS Publications website at DOI: ...

## 38 39 40 41 42 **Conflicts of Interest**

43 There are no conflicts of interest to declare.

## 44 45 46 47 **Acknowledgements**

48 This work was supported by the Russian Foundation for Basic Research (projects No 17-03-00035 and  
49 No 20-03-00112). XRD studies were performed by Drs. Kyrill Y. Suponitsky (A. N. Nesmeyanov  
50 Institute of Organoelement Compounds, Moscow) and Olesya V. Khoroshilova (Center for X-Ray  
51 Diffraction Studies, St. Petersburg State University Research Park). We also thank Drs. Anna V.  
52 Tkachuk and Oleg N. Burov (Scientific and Educational Laboratory of Resonance Spectroscopy,  
53 Department of Natural and High Molecular Compounds Chemistry, Southern Federal University) for  
54  
55  
56  
57  
58  
59

1  
2 NMR measurements. The authors gratefully acknowledge the Wroclaw Centre for Networking and  
3 Supercomputing (WCSS) for computational facilities.  
4

## 5 6 **References**

- 7  
8 (1) Pauling, L.; Pauling, P. *Chemistry*; Freeman, W. H. & Co.: San Francisco, 1975, 792 p.  
9  
10 (2) (a) Malone, J. F.; Murray, C. M.; Charlton, M. H.; Docherty, R.; Laverty, A. J. X–H... $\pi$  (phenyl)  
11 interactions. Theoretical and crystallographic observations. *J. Chem. Soc., Faraday Trans.* **1997**,  
12 *93*, 3429–3436. (b) Burley, S. K.; Petsko, G. A. Amino-aromatic interactions in proteins. *FEBS*  
13 *Letters* **1986**, *203*, 139–143. (c) Steiner, T.; Koellner, G. Hydrogen bonds with  $\pi$ -acceptors in  
14 proteins: frequencies and role in stabilizing local 3D structures. *J. Mol. Biol.* **2001**, *305*, 535–557.  
15 (d) Fernandez-Recio, J.; Romero, A.; Sancho, J. Energetics of a hydrogen bond (charged and  
16 neutral) and of a cation- $\pi$  interaction in apoflavodoxin. *J. Mol. Biol.* **1999**, *290*, 319–330. (e)  
17 Perutz, M. F. The role of aromatic rings as hydrogen-bond acceptors in molecular recognition. *Phil.*  
18 *Trans. R. Soc. A* **1993**, *345*, 105–112. (f) Yao, H.; Ke, H.; Zhang, X.; Pan, S.-J.; Li, M.-S.; Yang,  
19 L.-P.; Schreckenbach, G.; Jiang, W. Molecular Recognition of Hydrophilic Molecules in Water  
20 by Combining the Hydrophobic Effect with Hydrogen Bonding. *J. Am. Chem. Soc.* **2018**, *140*,  
21 13466–13477. (g) Recently, the effect of NH... $\pi$  interaction has been successfully applied for the  
22 industrially important separation of the benzene, cyclohexene and cyclohexane mixture, which is  
23 formed at hydrogenation of benzene. Yao, H.; Wang, Y.-M.; Quan, M.; Farooq, M. U.; Yang, L.-P.;  
24 Jiang, W. Adsorptive Separation of Benzene, Cyclohexene, and Cyclohexane by Amorphous  
25 Nonporous Amide Naphthotubes Solids. *Angew. Chem. Int. Ed.* **2020**, DOI:  
26 10.1002/anie.202009436.  
27  
28  
29  
30  
31  
32  
33  
34  
35  
36  
37  
38  
39 (3) (a) Saloutina, L. V.; Zapevalov, A. Ya.; Saloutin, V. I.; Kodess, M. I.; Slepukhin, P. A. Reactions of  
40 internal perfluoroolefin oxides with urea. *Russ. J. Org. Chem.* **2009**, *45*, 865–871. (b) Zhao, Q.;  
41 Sun, H.; Chen, W.; Duan, C.; Liu, Y.; Pan, Yi; You, X. Synthesis and Structural Characterization of  
42 the Novel Compounds from the Reactions of Trimethylaluminum or Trimethylgallium with N,O-  
43 Donor Crown Ethers. *Organometallics* **1998**, *17*, 156–160. (c) Sidorov, A. A.; Fomina, I. G.;  
44 Malkov, A. E.; Reshetnikov, A. V.; Aleksandrov, G. G.; Novotortsev, V. M.; Nefedov, S. E.;  
45 Eremenko, I. L. Synthesis and structures of nickel(II) trimethylacetate dimers with coordinated  
46 diamines. *Russ. Chem. Bull.* **2000**, *49*, 1887–1890. (d) Mulford, D. R.; Fanwick, P. E.; Rothwell, I.  
47 P. Group 4 and 5 metal derivatives of 2,2'-methylene-bis(6-phenylphenoxide). *Polyhedron* **2000**,  
48 *19*, 35–42. (e) Fomina, I.; Dobrokhotova, Z.; Aleksandrov, G.; Bogomyakov, A.; Fedin, M.;  
49 Dolganov, A.; Magdesieva, T.; Novotortsev, V.; Eremenko, I. Influence of the nature of organic  
50  
51  
52  
53  
54  
55  
56  
57  
58  
59  
60

- 1 components in dinuclear copper(II) pivalates on the composition of thermal decomposition  
2 products. *Polyhedron* **2010**, *29*, 1734–1746. (f) Gröger, N.; Wadepohl, H.; Gade, L. H. Iridium  
3 Complexes Containing a PNP Pincer Ligand: Syntheses, Structural Chemistry, and Bond  
4 Activations. *Eur. J. Inorg. Chem.* **2013**, 5358–5365. (g) Tomaszewski, P.; Wiszniewski, M.;  
5 Serwatowski, J.; Woźniak, K.; Durka, K.; Lulinski, S. Synthesis of tetraarylbates *via* tetralithio  
6 intermediates and the effect of polar functional groups and cations on their crystal structures.  
7 *Dalton Trans.* **2018**, *47*, 16627–16637. (h) Steiner, T.; Mason, S. A. Short N<sup>+</sup>–H···Ph hydrogen  
8 bonds in ammonium tetraphenylborate characterized by neutron diffraction. *Acta Cryst., B*  
9 **2000**, *56*, 254–260. (i) Johnstone, T. C.; Briceno-Strocchia, A. I.; Stephan, D. W. Frustrated Lewis  
10 Pair Oxidation Permits Synthesis of a Fluoroazaphosphatane, [FP(MeNCH<sub>2</sub>CH<sub>2</sub>)<sub>3</sub>N]<sup>+</sup>. *Inorg.*  
11 *Chem.* **2018**, *57*, 15299–15304.
- 21 (4) (a) Ilioudis, C. A.; Bearpark, M. J.; Steed, J. W. Hydrogen bonds between ammonium ions and  
22 aromatic rings exist and have key consequences on solid-state and solution phase properties. *New J.*  
23 *Chem.* **2005**, *29*, 64–67. (b) Kim, S.-G.; Kim, K.-H.; Kim, Y. K.; Shin, S. K.; Ahn, K. H. Crucial  
24 Role of Three-Center Hydrogen Bonding in a Challenging Chiral Molecular Recognition. *J.*  
25 *Am. Chem. Soc.* **2003**, *125*, 13819–13824. (c) Lan, P.; Herlt, A. J.; Willis, A. C.; Taylor, W. C.;  
26 Mander, L. N. Structures of New Alkaloids from Rain Forest Trees *Galbulimima belgraveana*  
27 and *Galbulimima baccata* in Papua New Guinea, Indonesia, and Northern Australia. *ACS*  
28 *Omega* **2018**, *3*, 1912–1921. (d) Micheloni, M.; Formica, M.; Fusi, V.; Romani, P.; Pontellini, R.;  
29 Dapporto, P.; Paoli, P.; Rossi, P.; Valtancoli, B. Synthesis, Crystal Structures and Lithium  
30 Encapsulation by Some Phenolic Aza Cages. *Eur. J. Inorg. Chem.* **2000**, 51–57. (e) Zheng, S.-L.;  
31 Coppens, P. Emission quenching of photoactive molecules embedded in supramolecular solids:  
32 Synthesis, structure and photoluminescence studies of benzil in a CMCR-based inclusion complex  
33 with a saturated linker molecule. *CrystEngComm* **2005**, *7*, 289–293. (f) Nachtigall, F. F.; Vencato,  
34 I.; Lazzarotto, M.; Nome, F. Calix[4]arene Piperidinium Salt. *Acta Cryst., C* **1998**, *54*, 1007–1010.  
35 (g) Bachmann, J.; Teets, T. S.; Nocera, D. G. Proton storage in the periphery of zirconium(IV)  
36 porphyrinogen. *Dalton Trans.* **2008**, 4549–4551.
- 49 (5) Anslyn, E. V.; Dougherty, D. A. *Modern Physical Organic Chemistry*; University Science Books:  
50 Sausalito, CA, 2006, p 495.
- 53 (6) Quite a few articles are devoted to different aspects of NH...π *peri*-interactions between the  
54 protonated Me<sub>2</sub>N group and C=O and C=C bonds: (a) Mercadal, N.; Day, S. P.; Jarmyn, A.; Pitak,  
55 M. B.; Coles, S. J.; Wilson, C.; Rees, G. J.; Hanna, J. V.; Wallis, J. D. O- vs. N-protonation of 1-  
56  
57  
58  
59  
60

- 1 dimethylaminonaphthalene-8-ketones: formation of a *peri*-N-C bond or a hydrogen bond to the pi-  
2 electron density of a carbonyl group. *CrystEngComm*, **2014**, *16*, 8363–8374. (b) Wannebroucq, A.;  
3 Jarmyn, A. P.; Pitak, M. B.; Coles, S. J.; Wallis, J. D. Reactions and interactions between *peri*-  
4 groups in 1-dimethylamino-naphthalene salts: an example of a “through space” amide. *Pure and*  
5 *Applied Chemistry*, **2016**, *88*, 317–331. (c) Scerba, M. T.; DeBlase, A. F.; Bloom, S.; Dudding, T.;  
6 Johnson, M. A.; Lectka, T. Characterization of Highly Unusual NH<sup>+</sup>–O Hydrogen Bonding to Ester  
7 Ether Oxygen Atoms through Spectroscopic and Computational Studies. *J. Phys. Chem. A*, **2012**,  
8 *116*, 3556–3560. (d) Schweizer, W. B.; Procter, G.; Kaftory, M.; Dunitz, J. D. Structural Studies of  
9 1,8-Disubstituted Naphthalenes as Probes for Nucleophile-Electrophile Interactions. *Helv. Chim.*  
10 *Acta* **1978**, *61*, 2783–2808. (e) Asaad, N.; Davies, J. E.; Hodgson, D. R. W.; Kirby, A. J.; van Vliet,  
11 L.; Ottavi, L. The search for efficient intramolecular proton transfer from carbon: the kinetically  
12 silent intramolecular general base-catalysed elimination reaction of O-phenyl 8-dimethylamino-1-  
13 naphthaldoximes. *J. Phys. Org. Chem.* **2005**, *18*, 101–109.
- 14 (7) Pozharskii, A. F.; Ozeryanskii, V. A.; Filatova, E. A.; Dyablo, O. V.; Pogosova, O. G.; Borodkin,  
15 G. S.; Filarowski, A.; Steglenko, D. V. Neutral pyrrole nitrogen atom as a  $\pi$ - and mixed  $n,\pi$ -donor  
16 in hydrogen bonding. *J. Org. Chem.* **2019**, *84*, 726–737.
- 17 (8) Pozharskii, A. F.; Ozeryanskii, V. A.; Dyablo, O. V.; Pogosova, O. G.; Borodkin, G. S.; Filarowski,  
18 A. Nucleophilic substitution of hydrogen atom in initially inactivated pyrrole ring. *Org. Lett.* **2019**,  
19 *21*, 1953–1957.
- 20 (9) Jurok, R.; Cibulka, R.; Dvořáková, H.; Hampl, F.; Hodačová, J. Planar Chiral Flavinium Salts –  
21 Prospective Catalysts for Enantioselective Sulfoxidation Reactions. *Eur. J. Org. Chem.* **2010**,  
22 *5217–5224*.
- 23 (10) Nielsen, A. T.; DeFusco, A. A.; Browne, T. E. Nitration of bis(amido)naphthalenes. *J. Org.*  
24 *Chem.* **1985**, *50*, 4211–4218.
- 25 (11) Hull, K. L.; Sanford, M. S. Catalytic and Highly Regioselective Cross-Coupling of Aromatic C–H  
26 Substrates. *J. Am. Chem. Soc.* **2007**, *129*, 11904–11905.
- 27 (12) Dyablo, O. V.; Pozharskii, A. F.; Shmoilova, E. A.; Ozeryanskii, V. A.; Fedik, N. S.; Suponitsky,  
28 K. Yu. Molecular structure and protonation trends in 6-methoxy- and 8-methoxy-2,4,5-  
29 tris(dimethylamino)quinolines. *J. Mol. Struct.* **2016**, *1107*, 305–315.
- 30 (13) Pozharskii, A. F.; Ozeryanskii, V. A.; Mikshiev, V. Y.; Antonov, A. S.; Chernyshev, A. V.;  
31 Metelitsa, A. V.; Borodkin, G. S.; Fedik, N. S.; Dyablo, O. V. 10-Dimethylamino derivatives of  
32 benzo[*h*]quinoline and benzo[*h*]quinazolines: fluorescent proton sponge analogues with opposed  
33  
34  
35  
36  
37  
38  
39  
40  
41  
42  
43  
44  
45  
46  
47  
48  
49  
50  
51  
52  
53  
54  
55  
56  
57  
58  
59  
60

- 1  
2 *peri*-NMe<sub>2</sub>/-N= groups. How to distinguish between proton sponges and pseudo-proton sponges. *J.*  
3 *Org. Chem.* **2016**, *81*, 5574–5587.
- 4  
5 (14) (a) Kim, K.; Jung, Y.; Lee, S.; Kim, M.; Shin, D.; Byun, H.; Cho, S. J.; Song, H.; Kim, H.  
6 Directed C–H Activation and Tandem Cross-Coupling Reactions Using Palladium Nanocatalysts  
7 with Controlled Oxidation. *Angew. Chem. Int. Ed.* **2017**, *56*, 6952–6956. (b) The dication of salt **31**  
8 resembles an open book with the interplane angle of 119° between the two mean benzoquinoline  
9 fragments, which is obviously originates from the Coulomb repulsion of the two positive charges  
10 and allows external molecules to arrange closer within the “book pages” and strongly bifurcate the  
11 NH protons.
- 12  
13 (15) (a) The equality of the NH...M and NH...N distances for compound **5** (2.07 Å) is strongly  
14 contrasted with the similar parameters for salts **1–4**: 2.39–2.56 for NH...M against 2.05–2.08 Å for  
15 NH...C1' (Table 1). This means that the NH...π interaction in **1–4** is predominantly directed to the  
16 *ipso* atom C1'. As for **5**, the equal orientation of the NH proton to the ring centroid and to the  
17 nitrogen atom is a unique phenomenon in the pyrrole and indole series,<sup>8</sup> where usually NH...π  
18 interaction is directed to the ring C-atoms.<sup>15b–c</sup> In this regard, it was interesting to see how this  
19 circumstance affects the aromaticity of the pyrrole ring. Comparison of the XRD parameters for **5**  
20 with those for the related pyrrole base **38**<sup>15d</sup> (ESI, p. S32, Figure S46) discloses that in **5** a  
21 significant increase in ring bond alternation takes place testifying the pronounced decrease in  
22 aromaticity. (b) Goddard, R.; Heinemann, O.; Krüger, C. Pyrrole and a Cocrystal of 1*H*- and 2*H*-  
23 1,2,3-Triazole. *Acta Cryst.* **1997**, *C53*, 1846–1850. (c) Evans, D. A.; Borg, G.; Scheidt, K. A.  
24 Remarkably Stable Tetrahedral Intermediates: Carbinols from Nucleophilic Additions to  
25 N-Acylpyrroles. *Angew. Chem., Int. Ed.* **2002**, *41*, 3188–3191. (d) Avila, D. V.; Davies, A. G.;  
26 Tocher, D. A.; Truter, M. R. Structure of Three Di-pyrrole Compounds. *Acta Cryst.*  
27 **1991**, *C47*, 1662–1667.
- 28  
29 (16) Tamgho, I. S.; Engle, J. T.; Ziegler, C. T. The syntheses and structures of  
30 bis(alkylimino)isoindolines. *Tetrahedron Lett.* **2013**, *54*, 6114–6117.
- 31  
32 (17) McClinton, M. A.; McClinton, D. A. Trifluoromethylations and related reactions in organic  
33 chemistry. *Tetrahedron* **1992**, *48*, 6555–6666.
- 34  
35 (18) Pozharskii, A. F.; Zvezdina, E. A. The Acid Properties of the Amino-group. *Russ. Chem. Rev.*  
36 **1973**, *42*, 37–55.
- 37  
38 (19) Badger, G. M. *Aromatic Character and Aromaticity*. Cambridge University Press, 1969, p. 65.
- 39  
40  
41  
42  
43  
44  
45  
46  
47  
48  
49  
50  
51  
52  
53  
54  
55  
56  
57  
58  
59  
60

- (20) The existence of complex **32** in the solid state both inside and outside of supramolecular tubes has been also confirmed by XRD method.<sup>19</sup> Notably, the CH... $\pi$  distance in those greatly depends on the environment changing from 2.103 to 2.826 Å.
- (21) (a) Zong, J.; Mague, J. T.; Pascal, R. A. Exceptional Steric Congestion in an *in,in*-Bis(hydrosilane). *J. Am. Chem. Soc.* **2013**, *135*, 13235–13237. (b) Lakshminarayanan, P. S.; Kumar, D. K.; Ghosh, P. Solid State Structural Evidence of Chloroform–Benzene–Chloroform Adduct Trapped in Hexaanthryl Octaaminocryptand Channels. *J. Am. Chem. Soc.* **2006**, *128*, 9600–9601. (c) Pariya, C.; Sparrow, C. R.; Back, C.-K.; Sandi, G.; Fronczek, F. R.; Maverick, A. W. Copper  $\beta$ -Diketonate Molecular Squares and Their Host–Guest Reactions. *Angew. Chem., Int. Ed.* **2007**, *46*, 6305–6308.
- (22) Pfaffen, C.; Infanger, D.; Ottiger, P.; Frey, H.-M.; Leutwyler, S. N–H... $\pi$  hydrogen-bonding and large-amplitude tipping vibrations in jet-cooled pyrrole–benzene. *Phys. Chem. Chem. Phys.* **2011**, *13*, 14110–14118.
- (23) Howard, S. T. Relationship between Basicity, Strain, and Intramolecular Hydrogen-Bond Energy in Proton Sponges. *J. Am. Chem. Soc.* **2000**, *122*, 8238–8244.
- (24) (a) Reed, A. E.; Weinhold, F.; Curtiss, L. A.; Pochatko, D. J. Natural bond orbital analysis of molecular interactions: Theoretical studies of binary complexes of HF, H<sub>2</sub>O, NH<sub>3</sub>, N<sub>2</sub>, O<sub>2</sub>, F<sub>2</sub>, CO, and CO<sub>2</sub> with HF, H<sub>2</sub>O, and NH<sub>3</sub>. *J. Chem. Phys.* **1986**, *84*, 5687–5705. (b) Stone, A. J. Natural Bond Orbitals and the Nature of the Hydrogen Bond. *J. Phys. Chem. A* **2017**, *121*, 1531–1534.
- (25) (a) Palermo, N. Y.; Csontos, J.; Owen, M. C.; Murphy, R. F.; Lovas, S. Aromatic-backbone interactions in model  $\alpha$ -helical peptides. *J. Comput. Chem.* **2007**, *28*, 1208–1214. (b) van Mourik, T. Comment on “Aromatic-Backbone Interactions in Model  $\alpha$ -Helical Peptides” [Palermo et al., *J. Comput. Chem.* 2007, 28, 1208]. *J. Comput. Chem.* **2008**, *29*, 1–3.
- (26) Grimme, S.; Hansen, A.; Brandenburg, J. G.; Bannwarth, C. Dispersion-Corrected Mean-Field Electronic Structure Methods. *Chem. Rev.* **2016**, *116*, 5105–5154.
- (27) Wozniak, K.; Mallison, P. R.; Smith, G. T.; Wilson, C. C.; Grech, E. Role of C–H...O hydrogen bonds in the ionic complexes of 1,8-bis(dimethylamino)naphthalene. *J. Phys. Org. Chem.* **2003**, *16*, 764–771.
- (28) Becke, A. D. Density-functional thermochemistry. III. The role of exact exchange. *J. Chem. Phys.* **1993**, *98*, 5648–5652.
- (29) Lee, C.; Yang, W.; Parr, R. G. Development of the Colle-Salvetti correlation-energy formula into a functional of the electron density. *Phys. Rev. B* **1988**, *37*, 785–789.

- 1  
2 (30) (a) McLean, A. D.; Chandler, G. S. Contracted Gaussian basis sets for molecular calculations. I.  
3 Second row atoms,  $Z = 11-18$ . *J. Chem. Phys.* **1980**, *72*, 5639–5648. (b) Frisch, M. J.; Pople, J. A.;  
4 Binkley, J. S. Self-consistent molecular orbital methods. 25. Supplementary functions for Gaussian  
5 basis sets. *J. Chem. Phys.* **1984**, *80*, 3265–3269.  
6  
7  
8 (31) Gaussian 16, Revision B.01, Gaussian, Inc., Wallingford CT, 2016.  
9  
10 (32) (a) Grimme, S. Semiempirical GGA-type density functional constructed with a long-range  
11 dispersion correction. *J. Comput. Chem.* **2006**, *27*, 1787–1799. (b) von Lilienfeld, O. A.;  
12 Tkatchenko, A. Two- and three-body interatomic dispersion energy contributions to binding in  
13 molecules and solids. *J. Chem. Phys.* **2010**, *132*, 234109. (c) Grimme, S.; Antony, J.; Schwabe, T.;  
14 Mück-Lichtenfeld, C. Density functional theory with dispersion corrections for supramolecular  
15 structures, aggregates, and complexes of (bio)organic molecules. *Org. Biomol. Chem.* **2007**, *5*,  
16 741–758.  
17  
18 (33) Miertuš, S.; Scrocco, E.; Tomasi, J. Electrostatic interaction of a solute with a continuum. A direct  
19 utilizaion of AB initio molecular potentials for the prevision of solvent effects. *Chem. Phys.* **1981**,  
20 *55*, 117–129.  
21  
22 (34) Scalmani, G.; Frisch, M. J.; Mennucci, B.; Tomasi, J.; Cammi, R.; Barone, V. Geometries and  
23 properties of excited states in the gas phase and in solution: Theory and application of a time-  
24 dependent density functional theory polarizable continuum model. *J. Chem. Phys.* **2006**, *124*,  
25 094107.  
26  
27 (35) Tomasi, J.; Mennucci, B.; Cammi, R. Quantum Mechanical Continuum Solvation Models. *Chem.*  
28 *Rev.* **2005**, *105*, 2999–3094.  
29  
30  
31  
32  
33  
34  
35  
36  
37  
38  
39  
40  
41  
42  
43  
44  
45  
46  
47  
48  
49  
50  
51  
52  
53  
54  
55  
56  
57  
58  
59  
60